

# Nanostructured Design Cathode Materials for Magnesium-Ion Batteries

Mohsin Javed, Afzal Shah,\* Jan Nisar, Suniya Shahzad, Abdul Haleem, and Iltaf Shah\*

Cite This: *ACS Omega* 2024, 9, 4229–4245

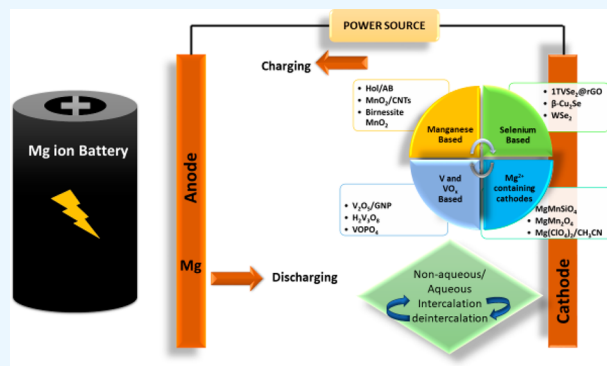
Read Online

ACCESS |

Metrics &amp; More

Article Recommendations

**ABSTRACT:** Energy is undeniably one of the most fundamental requirements of the current generation. Solar and wind energy are sustainable and renewable energy sources; however, their unpredictability points to the development of energy storage systems (ESSs). There has been a substantial increase in the use of batteries, particularly lithium-ion batteries (LIBs), as ESSs. However, low rate capability and degradation due to electric load in long-range electric vehicles are pushing LIBs to their limits. As alternative ESSs, magnesium-ion batteries (MIBs) possess promising properties and advantages. Cathode materials play a crucial role in MIBs. In this regard, a variety of cathode materials, including Mn-based, Se-based, vanadium- and vanadium oxide-based, S-based, and Mg<sup>2+</sup>-containing cathodes, have been investigated by experimental and theoretical techniques. Results reveal that the discharge capacity, capacity retention, and cycle life of cathode materials need improvement. Nevertheless, maintaining the long-term stability of the electrode–electrolyte interface during high-voltage operation continues to be a hurdle in the execution of MIBs, despite the continuous research in this field. The current Review mainly focuses on the most recent nanostructured-design cathode materials in an attempt to draw attention to MIBs and promote the investigation of suitable cathode materials for this promising energy storage device.



## 1. INTRODUCTION

The rising world population is predicted to reach 10 billion by 2058. Around 80% of the global population is expected to be residents of cities by 2050. Urban areas occupy 2% of the Earth's surface, while cities utilize more than 75% of the world's natural resources. This leads to extensive globalization and consequent adverse effects on humans.<sup>1,2</sup> The demand for nonrenewable energy sources such as fossil fuels has exponentially increased due to technological advancements and resource constraints brought by the increasing population.<sup>3,4</sup> The use of such resources has caused serious ecological and environmental problems. The detrimental effects of hydrocarbon emissions, carbon dioxide, oxides of nitrogen and sulfur, and continuous depletion of fossil fuels have led scientists to focus on renewable energy sources.<sup>5</sup> In this regard, hydropower, biomass, solar, wind, geothermal, and hydrogen energies are receiving particular attention owing to their ecologically beneficial qualities along with their capacity to generate energies with zero or virtually zero emission of pollutants.<sup>6,7</sup> Solar, wind, hydropower, and geothermal energies are constantly being generated; however, these sources are unpredictable and less reliable due to seasonal and even daily changes. For instance, weather fluctuations greatly impact solar radiation strength and the voltage and

frequency of wind generation. A solar panel may not function properly in cloudy weather, and wind turbines may not work in fair weather. Additionally, these sources sporadically generate excessive energy, which causes overload in the system. This inconsistency in the supply can be overcome with affordable and efficient energy storage systems (ESSs).

ESSs are considered to have the potential for optimal energy management as well as regulating energy spillage and maintaining the balance between energy supply and consumption. ESSs are primarily prepared to get energy from multiple sources, the convert and store it for diverse uses as needed.<sup>8</sup> ESSs can be categorized on the basis of the type of energy stored, the duration of storage, and the efficiency of storage. Energy is stored in variety of forms, such as electrochemical, mechanical, thermal, chemical, magnetic, and electric fields.<sup>9</sup> ESSs have the potential to absorb and

Received: September 1, 2023

Revised: December 7, 2023

Accepted: December 22, 2023

Published: January 19, 2024

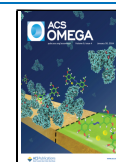


Table 1. A Brief Comparison of Li-Ion and Mg-Ion Batteries

feature	Li-ion batteries	Mg-ion batteries
cathode material	lithium cobalt oxide (LiCoO <sub>2</sub> ), lithium iron phosphate (LiFePO <sub>4</sub> ), or others are typically used	utilize magnesium intercalation compounds
anode material	graphite is commonly used	magnesium metal or magnesium alloys
energy density	high energy density	potentially higher energy density than Li-ion
specific energy	generally lower than Mg-ion batteries	higher specific energy per unit mass
cycle life	good cycle life, but degrades over time	cycle life may still be improving
charging speed	fast charging capabilities	charging speed improvements are underway
safety	generally safe, but some risk of thermal runaway	potentially safer due to magnesium's nature
cost	relatively mature technology; cost-effective	still in development; may be costlier
commercialization	widely used in various applications	still in the research and development stage
environmental impact	lithium extraction and disposal can have impacts	magnesium is more abundant and less toxic

release energy across a range of time intervals, hence facilitating the increased penetration of renewable energy. Researchers are curious about the battery energy storage systems (BESSs) because of the obvious advantages they offer, such as fast reaction, controllability, and independence from geographic location.<sup>10</sup>

Batteries are electrochemical devices that transform chemical energy into electrical energy. They are made up of several cells, all of which have three essential parts: an electrolyte and two electrodes (an anode and a cathode).<sup>11</sup> In many aspects of modern life, batteries provide an infinite number of advantages. For instance, they provide transportable power to a variety of portable gadgets such as cellphones, cameras, tablets, and wearable gadgets.<sup>12</sup> The power storage of batteries harvested from solar and wind sources can be used in cloudy or calm weather, i.e., when the sun is not shining or wind is not blowing. In times of crises or power outages, batteries offer a dependable source of backup power. They may be used to support hospitals, telecommunications, critical infrastructure, and other vital services, assuring operational continuity and safety under challenging conditions.<sup>13</sup> Grid flexibility is another benefit of large-scale battery systems owing to their ability to keep a balance between demand and supply and maintain grid stability by storing extra power during times of low demand and releasing it during times of excessive need.<sup>14</sup> Batteries have ecological benefits, as they can contribute to lowering the greenhouse effect and air pollution. When used in electric vehicles (EVs), batteries do not produce exhaust emissions, unlike fossil fuels, and hence their usage is effective against climate change.<sup>15</sup> Batteries can reduce or eliminate power plants powered by fossil fuels to produce electricity. They allow for the harvesting and storage of lost electricity, thus supporting more effective use of the generated power.<sup>16</sup> By converting kinetic energy into electrical energy and storing it in the battery during regenerative braking, for instance, hybrid and electric vehicles can save their overall energy costs. These can also reduce noise.<sup>17</sup> In fact, devices and vehicles powered by batteries are often quieter than those driven by internal combustion engines. In particular, in metropolitan areas this may have a positive effect on lowering noise pollution.<sup>18</sup> Although the initial price of batteries may be high, they can result in long-term cost savings. For instance, pairing batteries with solar panels can eventually result in lower electricity costs and less dependence on the grid. The running expenses of electric vehicles, including gasoline and maintenance, are

frequently lower than those of typical internal combustion engine automobiles.<sup>19</sup>

Batteries may be primary or secondary. The chemicals of primary batteries cannot be recycled once used. Metal–air depolarized batteries, Zn–C cells, and alkaline Zn–MnO<sub>2</sub> cells are a few examples of such batteries. On the other hand, secondary batteries are designed to be recharged, for instance, Ni–metal hydride batteries, Ni–Cd batteries, Li-ion batteries (LIBs), Mg-ion batteries (MIBs), Zn-ion batteries, and Al-ion batteries.<sup>20,21</sup> LIBs are favored over other types of batteries for a variety of reasons, such as durability, lower cost, and high energy density. Primarily, they can store more energy in smaller, lighter packaging because of their high energy density, which makes them perfect for mobile devices such as cell phones and laptops. Second, LIBs have a longer life span and may endure hundreds of charge–discharge cycles without suffering appreciable capacity loss. They become more cost-effective in the long run. LIBs may hold a charge for a long time even when they are not being used because of their low self-discharge rate. They are also susceptible to a memory effect; there is no requirement for full discharge before recharging. They can be charged quickly due to their high charge acceptance rate.<sup>22,23</sup> Their portability and low weight make them useful in numerous fields, including renewable energy storage systems, electric vehicles, and consumer electronics. Besides all of these advantages, LIBs are associated with certain limitations. First, because extraction and purification procedures are expensive, the price and supply of lithium resources may be constrained. Overheating and thermal runaway are additional safety concerns with LIBs that can lead to fires or explosion.<sup>24–28</sup> Other factors include the effect of lithium extraction and battery disposal on the environment. Owing to these limitations, researchers are looking into MIBs as a potential solution to these problems and to equip the market with this energy storage device.

## 2. MG-ION BATTERIES

MIBs have numerous advantages. Due to their many advantages over conventional LIBs, MIBs are quickly becoming a viable substitute for these batteries in a variety of applications.<sup>29</sup> The high energy density of MIBs is one of the main benefits. Compared with lithium, magnesium has a higher volumetric energy density. This means that MIBs can store more energy per unit volume, allowing for more energy storage capacity in a smaller and more compact battery

system.<sup>30</sup> In applications where storage is at a premium, such as in EVs and renewable energy storage systems, this is a tremendous asset. The enhanced safety profile of MIBs is another noteworthy advantage. Safety issues with LIBs have been addressed, including the possibility of thermal runaway and fire or explosion.<sup>31</sup> On the other side, magnesium is a more stable and passive element, which lessens the possibility of such safety events. By reducing these dangers, the use of magnesium in batteries is a safer option for consumer electronics, storing energy from renewable energy sources, and automotive applications.<sup>32</sup> Magnesium is abundantly available for the long-term viability of MIBs. In contrast to lithium, which can only be collected from restricted stocks, magnesium can also be obtained from a variety of sources, including saltwater and brine.<sup>33</sup> Because of its ease of access and abundance, magnesium is a cost-effective and ecologically beneficial option for substantial battery production. By lowering demands on rare metals and other materials, MIBs can facilitate the shift toward a greener, renewable energy future.<sup>34</sup> MIBs exhibit good electrochemical performance, including high charge–discharge efficiency, enabling efficient energy conversion and usage. Because of their high tolerance for charge and discharge cycles, MIBs have a rather long cycle life.<sup>35</sup> This durability is critical for situations where batteries must withstand repeated use while maintaining their performance over an extended period. In addition, MIBs have the potential for great power output. They have fast charging, which makes them ideal for applications requiring quick energy replenishment. This feature is especially useful for electric vehicles, where quick charging capacities are utilized to cut charging periods and boost consumer satisfaction.<sup>36</sup> A brief comparison of Li-ion and Mg-ion batteries is given in Table 1.

Magnesium ions can intercalate and deintercalate inside the host electrode material, making MIBs work. Electrolytes move  $Mg^{2+}$  ions from the cathode (positive electrode) to the anode (negative electrode) during charging and vice versa. To store electrical energy, the process is made possible by the flow of electrons in an external circuit. The magnesium ions return to the electrode once the battery is depleted, discharging their stored energy.<sup>37,38</sup> MIBs demand stable electrode materials that can accommodate the reversible intercalation of these ions, as well as an electrolyte that can efficiently transport magnesium ions for efficient battery operation. The cathode materials in Mg-ion batteries are essential to the battery's overall effectiveness and efficiency.<sup>39</sup> During the charge and discharge processes, the cathode is responsible for reversible intercalation or alloying of magnesium ions. To provide effective energy storage and retrieval, the material should have a large capacity to store and release magnesium ions, good cycling stability, and low voltage hysteresis. The scarcity of materials that are ideal for MIBs cathodes is one of the main drawbacks. The greater size of the magnesium ion makes the intercalation and combination with ordinary cathode materials quite difficult, which is the main cause of this constraint.<sup>40,41</sup>

This Review mainly focuses on cathode materials for MIBs, especially those based on a nanostructured design, and some density functional-based (DFT) studies of cathode materials, along with their crucial role in the development of battery technology. Numerous bulk and organic-based cathode materials have also been reported so far, but nanostructured cathode materials are preferred over them for several reasons. First, their enormous surface area improves charge/discharge rates and electrochemical performance. Second, the nanostruc-

ture makes it possible for them to have greater energy densities by increasing the number of active sites for Mg-ion intercalation. Third, because of decreased strain during cycling, the nanostructured material shows enhanced cyclic stability and electrode integrity. Additionally, the qualities of the nanostructures can be modified to perfection for targeted use. The subsequent section discusses the requirement of cathode materials, focusing on their high energy density, high specific capacity, charge/discharge capacity, cyclic stability, and the requirement for rapid magnesium-ion diffusion rates.

### 3. CATHODE MATERIALS FOR MG-ION BATTERIES

Due to magnesium's abundance and low cost as a raw material, MIBs are a potential alternative to LIBs.<sup>42</sup> However, various issues must be fixed before they can be commercially viable. One of the major challenges is the synthesis of suitable cathode materials due to the high charge density of  $Mg^{2+}$ , which makes the intercalation behavior more complex during charge and discharge cycles.<sup>43–45</sup> Furthermore, the selection of cathode materials is constrained due to challenges associated with intercalating magnesium-ions into several host structures.<sup>46</sup> Some of the other problems associated with cathode materials for MIBs are their instability, poor conductivity, and the slow diffusion kinetics of Mg-ions. In addition, cathode materials for MIBs typically suffer from poor cycle life, low rate capability, and low energy density.<sup>47</sup>

**3.1. Nanostructured Cathode Materials for Mg-Ion Batteries.** Some of these problems can be solved by making nanostructures with a large surface area for ion diffusion, shortening the paths for ion diffusion, and improving the interaction between electrodes and electrolytes.<sup>48</sup> Cathode materials for Mg-ion batteries should be designed with the following nanostructure aspects in mind.

The size and morphology of the cathode material play critical roles in the electrochemical performance of the MIBs. Nanostructured materials with a high surface area-to-volume ratio can provide more active sites for the intercalation and deintercalation of  $Mg^{2+}$  ions. Moreover, 1D and 2D nanomaterials can facilitate ion diffusion along specific directions and shorten the ion diffusion path.<sup>49</sup> The crystal structure of the cathode material can affect the  $Mg^{2+}$  ion intercalation and deintercalation process. For example, layered cathode materials have shown promising electrochemical performance due to their ability to intercalate  $Mg^{2+}$  ions between the layers.<sup>40</sup> Surface modification of the cathode material can enhance the interaction between the electrode and electrolyte, improve the conductivity of the electrode, and prevent the formation of an unwanted solid–electrolyte interface layer. Surface functionalization with organic or inorganic materials can improve the electrochemical performance of the cathode material.<sup>50</sup> The combination of different cathode materials or the incorporation of other materials into the cathode can lead to an enhanced electrochemical performance. For example, the incorporation of carbon nanotubes into the cathode material can improve electronic conductivity and prevent the mechanical degradation of the electrode.<sup>51</sup>

Nanostructured cathode materials for MIBs present a compelling avenue for enhancing the electrochemical performance of these energy storage devices. The implementation of nanostructured materials capitalizes on their inherent properties, such as high surface area, which facilitates rapid ion diffusion and significantly improves the kinetic aspects of charge and discharge cycles.<sup>52</sup> This larger surface area also

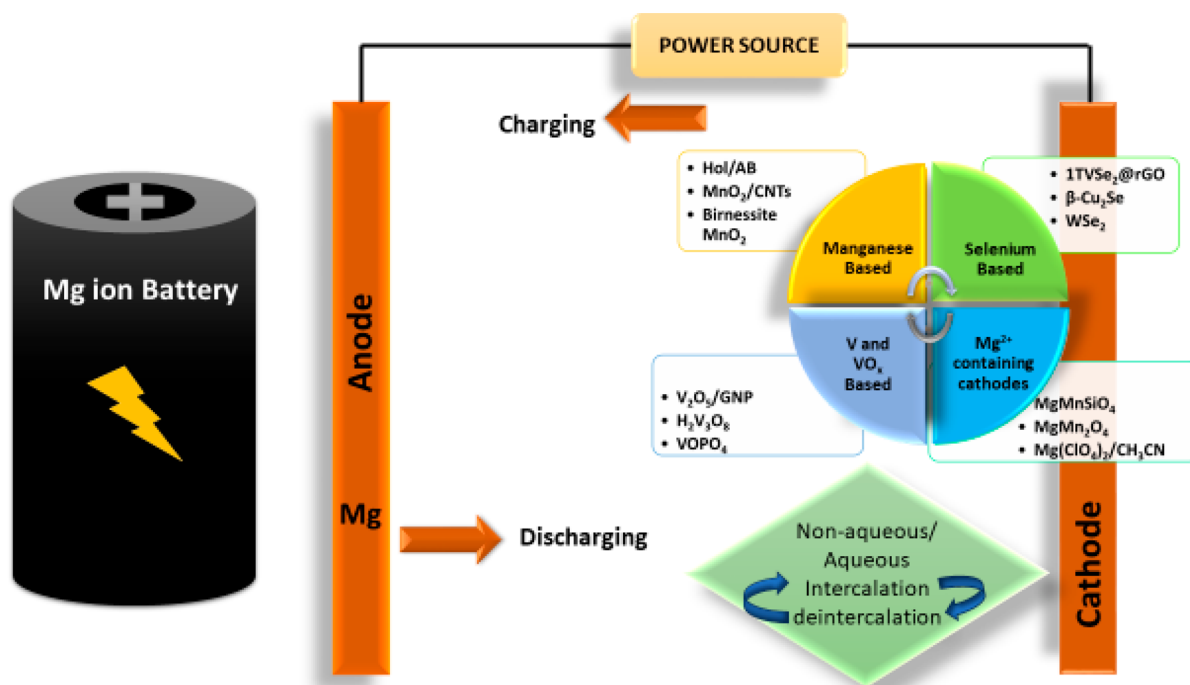


**Figure 1.** Pictorial illustration of MIBs along with different cathode materials.

offers an increased number of active sites for Mg-ion insertion and extraction, thereby augmenting the cathode's overall capacity and cycling stability. Additionally, nanostructured materials often foster better electrode–electrolyte interactions, promoting efficient ion transport and reducing the impedance at the electrode–electrolyte interface. This can contribute to better thermal stability, mitigating the risks of thermal degradation during battery operation.<sup>53</sup> However, challenges exist in the synthesis of nanostructured materials, as sophisticated methods are often required, impacting scalability and cost-effectiveness. Structural stability concerns over extended cycling, limited material choices, compatibility issues with other battery components, and the cost of production pose notable drawbacks.<sup>54</sup> Overcoming these challenges is crucial for realizing the full potential of nanostructured cathode materials in MIBs and for advancing the prospects of these batteries for sustainable energy storage solutions. Ongoing research endeavors aim to address these limitations and pave the way for the practical implementation of nanostructured designs in next-generation energy storage systems.

One promising strategy for improving the electrochemical performance of MIBs is the use of a nanostructured design for the cathode materials. To increase the kinetic features of charge and discharge cycles, inherent properties of nanostructured materials are used, such as a high surface area allowing rapid ion diffusion.<sup>55</sup> The capacity and cycle stability of the cathode are both improved as a result of the increased surface area, which provides more active sites for Mg-ion insertion and extraction. More efficient ion transport and lower impedance at the electrode–electrolyte interface are two additional benefits of nanostructured materials. This may aid in improved thermal stability, decreasing the likelihood of thermal damage in battery use.<sup>56</sup> Synthetic difficulties of nanostructured materials might have an effect on the materials' scalability and economic viability. Major limitations include the high cost of production, compatibility challenges with other

battery components, restricted material options, and worries about structural integrity after extended cycling.<sup>57,58</sup> To realize the full potential of nanostructured cathode materials in Mg-ion batteries and to further the prospects of these batteries as sustainable energy storage systems, we must overcome these obstacles must be overcome. Researchers are working to find solutions to these problems so that nanostructured designs can be used in real energy storage applications.

Overall, nanostructure design can be a promising strategy to overcome the challenges of developing efficient cathode materials for MIBs. However, the design of cathode materials for MIBs is still in its infancy, and further research is needed to optimize the electrochemical performance of MIBs. **Figure 1** illustrates the schematic representation of working of MIBs with magnesium as an anode and various nanostructured design materials as the cathode. These cathode materials are discussed in subsections along with their charge–discharge capacities and Coulomb efficiencies depending upon Mg to Mg<sup>2+</sup> conversion and the intercalation–deintercalation mechanism.

**3.2. Manganese-Based Cathode Materials.** A nanosized  $\alpha$ -MnO<sub>2</sub> cathode having a reversible capacity of over 240 mAh g<sup>-1</sup> for MIBs was studied by Arthur and co-workers using X-ray absorption spectroscopy (XAS) and X-ray photoelectron spectroscopy (XPS). The oxidation state of Mn-ions can change from less oxidized to more oxidized by the redox reaction of  $\alpha$ -MnO<sub>2</sub>, as evidenced by X-ray absorption near edge structure (XANES) and XPS spectra. Results from surface-probing XPS and bulk-averaging XANES were in good agreement with those from Extended X-ray absorption fine structure (EXAFS), which revealed local structural changes in the material. Furthermore, it established a connection between the permanent and partial breakdown of certain channel architectures and permanent loss of capacity during first cycle.<sup>59</sup> Rasul et al. synthesized electrode materials, namely, nanoscale hollandite-MnO<sub>2</sub> and haollandite-MnO<sub>2</sub>/acetylene

black (Hol/AB), and characterized them electrochemically. The Hol/AB [MnO<sub>2</sub>] combination was twice as powerful as pure hollandite, having an initial discharge capacity of 210 mAh g<sup>-1</sup>. Based on electrochemical performance, Hol/AB [MnO<sub>2</sub>] is predicted to be promising electrode material for MIBs, having a high rate capacity.<sup>60</sup> Later, Wang et al. demonstrated that sponge-shaped Mn<sub>3</sub>O<sub>4</sub> nanoparticles can serve as a cathode material in MIBs by using graphite foil as a current collector. The material exhibited high Coulombic efficiency and strong cyclic stability, which had been attributed to the network, its interconnected mesopores, widely dispersed nanoparticles (10 nm), and immense active surface area of 102 m<sup>2</sup> g<sup>-1</sup>. The study recommended further research on spinel host materials for MIBs.<sup>61</sup>

In another research study, the effect of electrolysis conditions on the electrochemical precipitation of MnO<sub>2</sub>/carbon nanotube (CNT) composites on stainless steel (SS 304) anode electrodes were investigated. MnO<sub>2</sub>/CNTs were synthesized, and field emission scanning electron microscopy (FESEM) revealed that the composite contained a crystalline phase of MnO<sub>2</sub> akhtenskite and CNTs. The composite's specific capacity was 92 mAh g<sup>-1</sup>, and after 35 charge-discharge cycles it retained 75% of its initial capacitance.<sup>62</sup> Because Mg<sup>2+</sup> is bivalent, it is challenging to produce high-voltage cathode materials with favorable deintercalation kinetics. Since the electrostatic contact between Mg<sup>2+</sup> ions and the host anion is a problem, crystal water was included in the layered structure of birnessite MnO<sub>2</sub> to mitigate it. The key role played by the crystal water was studied by Nam et al. with aberration-corrected scanning transmission electron microscopy (STEM). Working with water including nonaqueous electrolytes revealed the necessity of reducing the cathode–electrolyte interface desolvation energy penalty. After taking 1000 cycles of birnessite MnO<sub>2</sub> at 2.8 V vs Mg/Mg<sup>2+</sup> in aqueous electrolytes, a high reversible capacity of 231.1 mAh g<sup>-1</sup> was measured along with excellent cycle life and 62.5% capacity retention. All these were attributed to superior charge barrier in the host and effortless Mg<sup>2+</sup> ions transfer via the cathode's interface.<sup>63</sup>

Several Mn-based cathode materials were investigated based on their electrochemical performance. Hol/AB [MnO<sub>2</sub>] exhibited good initial discharge capacity, which was twice that of pure hollandite MnO<sub>2</sub>. Nanosized  $\alpha$ -MnO<sub>2</sub> showed promising reversible capacity. Mn<sub>3</sub>O<sub>4</sub> nanoparticles offered high Coulombic efficiency and good cyclic stability. MnO<sub>2</sub>/CNT composites showed good electrochemical performance, along with high capacity retention. Among the Mn-based cathode materials, all of them showed good electrochemical characteristics, but birnessite MnO<sub>2</sub> was prominent. However, the other cathode materials can be used according to the specific needs. Figure 2 presents the crystal structures of the nanostructured design cathode materials for MIBs.

**3.3. Selenium-Based Cathode Materials.** Liu et al. synthesized WSe<sub>2</sub> nanowire-assembled films and utilized them in MIBs as cathode materials. The electrode has excellent rate capability, enhanced specific capacity, and effective Mg<sup>2+</sup> intercalation.<sup>64</sup> A recent effort by Wei and his team described Ni<sub>3</sub>Se<sub>4</sub> as a unique cathode material for MIBs due to its ability to store up to 1 mol of Mg<sup>2+</sup>. However, it presented a significant migratory energy barrier, which was an issue. However, when synthesized hydrothermally, the resulting material had a discharge capacity of 99.8 mAh g<sup>-1</sup> at a current density of 50 mA g<sup>-1</sup>, and it retained 75% of its original

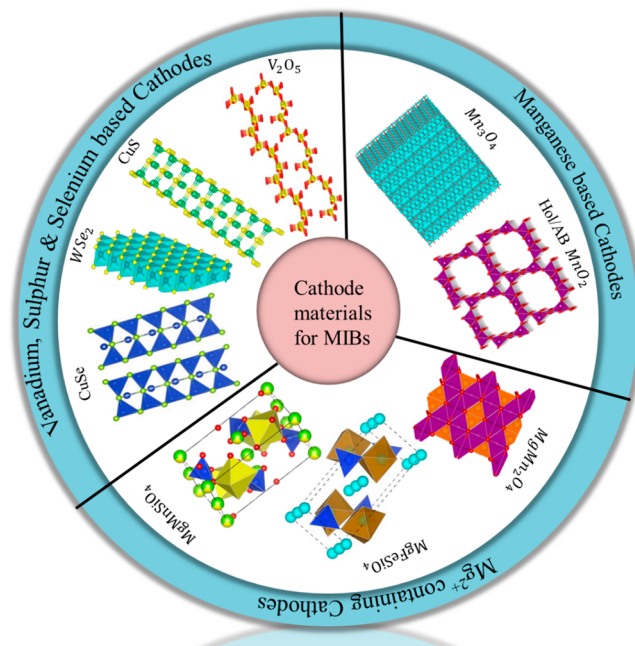
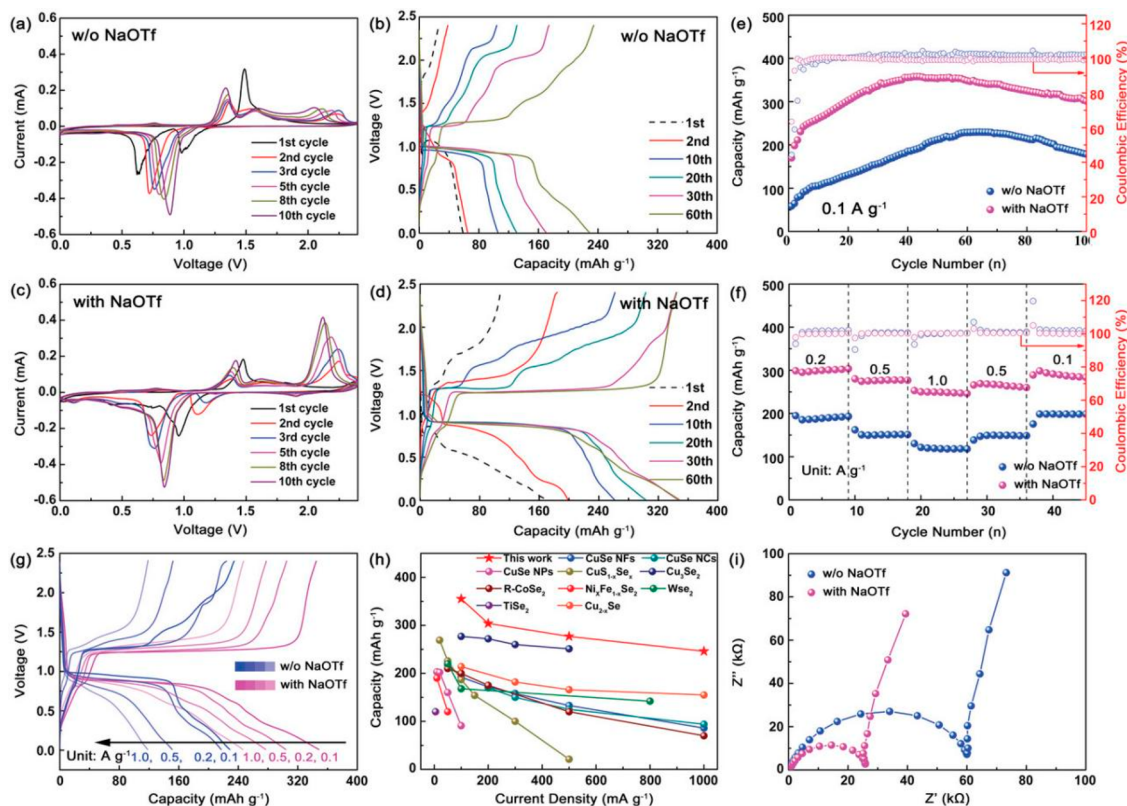


Figure 2. Nanostructured design of cathode materials for MIBs.

capacity after being cycled 100 times.<sup>65</sup> In a recent study, the cathode material WSe<sub>2</sub> nanosheet, shaped like a flower, was synthesized in a one-step hydrothermal process by Xu et al. and evaluated for use in MIBs. The reversible capacity of the WSe<sub>2</sub> cathode was greater than 265 mAh g<sup>-1</sup> at 50 mA g<sup>-1</sup>, and the rate capability was greater than 70% of the initial capacitance at 500 mA g<sup>-1</sup>. Support for WSe<sub>2</sub> as a cathode material for MIBs was found in this study.<sup>66</sup> In a recent effort under the supervision of Guoqiang Li, hydrothermal synthesis was employed to produce a composite of 1T-VSe<sub>2</sub> (1T vanadium diselenide) nanoparticles and reduced graphene oxide (1T-VSe<sub>2</sub>@rGO) for use as the cathode material for MIBs. The 1T-VSe<sub>2</sub>@rGO cathode demonstrated an excellent reversible capacity (235.5 mAh g<sup>-1</sup> at 50 mA g<sup>-1</sup>), a remarkable cycle life (62.7% of the initial capacitance was preserved after 500 cycles at 50 mA g<sup>-1</sup>), and a rate capability of 46% of the initial capacitance at 1000 mA g<sup>-1</sup>.<sup>67</sup>

A recent study by Zhao and his team modified the solvation structure of magnesium ions by introducing an anion to the electrolyte composition to facilitate Mg-ion storage processes. The trifluoromethanesulfonate anion, when added to a Mg-ion electrolyte, changes the solvation structure of Mg<sup>2+</sup>, hence increasing the rate of charge transfer from the cathode to the anode. Using CuSe as the cathode material on a Cu current collector significantly improved the magnesium storage capacity from 61% (228 mAh g<sup>-1</sup>) to 95% (357 mAh g<sup>-1</sup>) of the theoretical capacity at a low current density of 0.1 Ag<sup>1-</sup>, and it more than doubled at a high current density of 1.0 Ag<sup>1-</sup>. This study presented a feasible strategy for generating a high-rate conversion-type cathode material for MIBs through electrolyte modification.<sup>68</sup> Tashiro et al. reported that MIBs with a  $\beta$ -Cu<sub>2</sub>Se cathode achieved rechargeable performance. As a prototype cathode material for Mg batteries, the average specific capacity was close to 120 mAh g<sup>-1</sup> during the first 35 cycles at room temperature, placing it in close competition with the Chevrel phase. By reducing the size of the  $\beta$ -Cu<sub>2</sub>Se crystals to around 100 nm a side, the specific capacity was increased to around 230 mAh g<sup>-1</sup>. Incorporated Mg ions



**Figure 3.** Cyclic voltammetric curves of CuSe cathodes using the Mg-ion electrolytes at a  $0.1 \text{ mV s}^{-1}$  sweep rate (a) without or (b) with the NaOTf additive. Measurement of charge–discharge profiles of CuSe cathodes in electrolytes (c) without or (d) with NaOTf at a specific current of  $0.1 \text{ Ag}^{-1}$ . (e) Cycle life measurement at  $0.1 \text{ Ag}^{-1}$  and (f) rate measurement of CuSe cathodes. (g) Charge–discharge profiles of CuSe cathodes at varying current densities. (h) Comparison of the rate performance of Mg-ion storage cathode materials in this work with those of previous reports. (i) Nyquist plots of CuSe cathodes in different electrolytes after a rest period of 10 h. Reprinted with permission from ref 68. Copyright 2023 John Wiley and Sons.

promote the displacement and extrusion of Cu ions from Se sublattices, which has been thought as the mechanism for the reversible electrochemical reaction at the cathode. In this procedure, it was assumed that  $\beta\text{-Cu}_2\text{Se}$  and MgSe are structurally comparable.<sup>69</sup>

The WSe<sub>2</sub> nanowire film showed enhanced electrochemical properties. Ni<sub>3</sub>Se<sub>4</sub> showed an excellent cycle life and capacity retention. The WSe<sub>2</sub> nanosheet showed an effective discharge capacity and superb rate capability. The other Se-based cathodes include CuSe and  $\beta\text{-Cu}_2\text{Se}$ . Among Se-based cathode materials, CuSe is promising to be utilized as cathode material for MIBs because of its high discharge capacity. Figure 3 presents CV curves, discharge and charge profiles, and other electrochemical properties of CuSe. The other Se-based cathode materials can be used depending on the specific requirements.

**3.4. Vanadium- and Vanadium Oxide-Based Cathode Materials.** Kim et al., using a microwave-assisted hydrothermal method and an organic template, synthesized vanadium nanotubes of varying oxidation states ( $\text{V}^{3+}/\text{V}^{4+}/\text{V}^{5+}$ ).  $\text{V}^{3+}$  ions formed in highly reduced  $\text{VO}_x$  nanotubes were responsible for the high initial discharge capacity (over  $200 \text{ mAh g}^{-1}$ ) and excellent cycling behavior. These nanotubes have better cycling performance and lower charge transfer resistance than  $\text{VO}_x$  nanotubes with a reduced number of vanadium ions. The kinetics of magnesium insertion and extraction were shown to be highly dependent on the oxidation state and bonding structure of the nanotube surface. Using

$\text{VO}_x$  nanotubes as the cathode material, the study presented a radical approach to making magnesium-based rechargeable batteries with high energy density.<sup>70</sup> Tepavcevic and her lab fellows, after thorough research, used carbon nanofoam as a substrate for the electrochemical deposition of bilayered  $\text{V}_2\text{O}_5$ , which included hydroxyl groups and structural water for stabilization and cation preferences for  $\text{Mg}^{2+}$ . With a specific capacity of  $240 \text{ mAh g}^{-1}$  against a Mg anode, the electrode demonstrated reversible  $\text{Mg}^{2+}$  intercalation–deintercalation in an acetonitrile electrolyte. Imaging with high-resolution transmission electron microscopy (HRTEM) and X-ray fluorescence spectroscopy (XRF) showed that Mg ions were effectively inserted and removed during charging and discharging, correlating with the electrode capacity. The capacity of the anode validated the intercalation mechanism after the complete cell was rebuilt using a high-energy ball-milled Sn alloy anode.<sup>71</sup>

Improved electrical performance is attributed to the combination of  $\text{V}_2\text{O}_5$  and graphene nanoparticles (GNPs) in the  $\text{V}_2\text{O}_5/\text{GNP}$  cathode, which was manufactured by using a ball mill technique. Sheha et al. opened up new possibilities for cathode materials in MIBs using the high capacities of the above prepared  $\text{V}_2\text{O}_5$  and  $\text{V}_2\text{O}_5/\text{GNP}$  cathodes, which are  $100$  and  $90 \text{ mAh g}^{-1}$ , respectively.<sup>72</sup> Later, in a cell-configuration system, orthorhombic  $\text{V}_2\text{O}_5$  nanowires were produced and employed as cathodes, together with the  $\text{Mg}_x\text{Mo}_6\text{S}_8$  anode and  $1 \text{ M Mg}(\text{ClO}_4)_2$  electrolyte. With an initial discharge capacity ( $103 \text{ mAh g}^{-1}$ ) and charge capacity ( $110 \text{ mAh g}^{-1}$ ), the

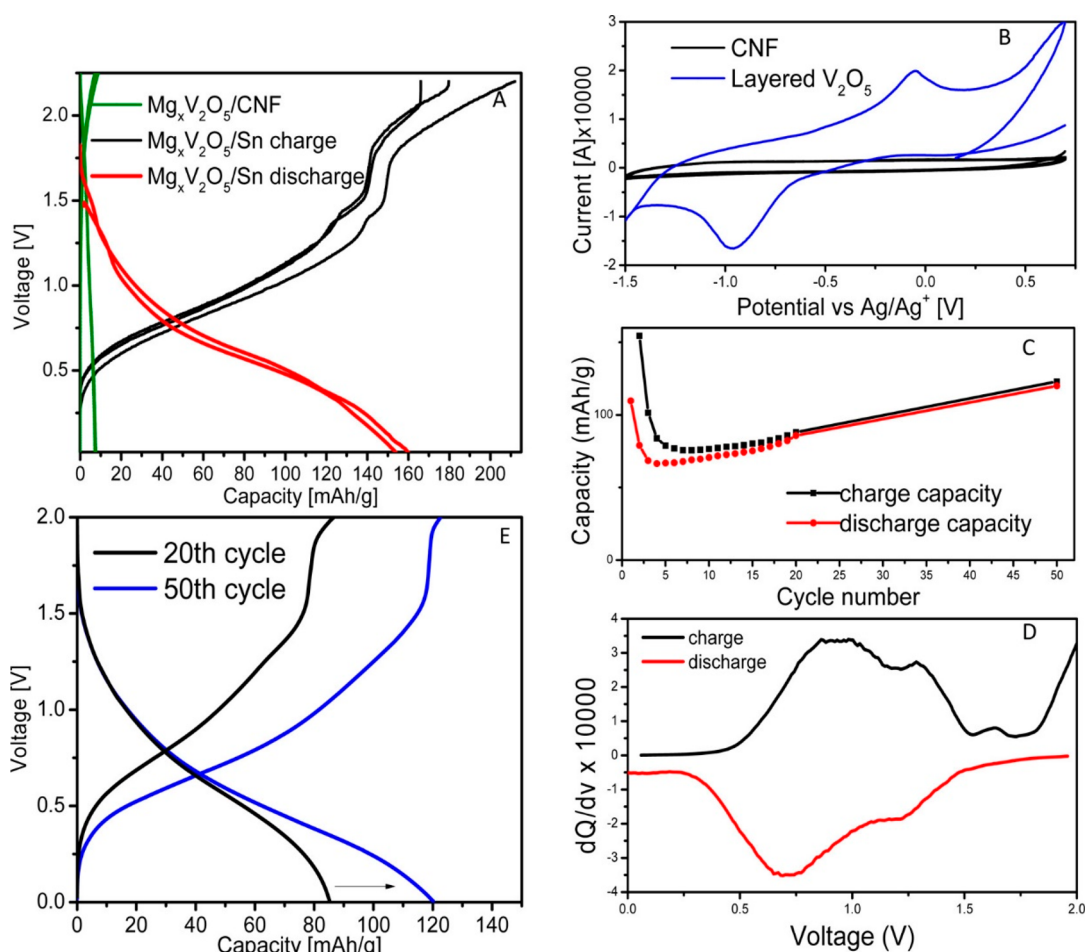


**Figure 4.** Electrochemical performance of a bilayered V<sub>2</sub>O<sub>5</sub> cathode. (a) First three charge–discharge cycles of Mg-enriched bilayered V<sub>2</sub>O<sub>5</sub> vs monocrystalline Sn electrode. Curves for charge–discharge cycles for same cathode vs CNF (a hard carbon disordered material) as the anode are shown (in green) for comparison. Both cells were cycled within the potential window of 2.2–0.0 V (vs Mg/Mg<sup>2+</sup>) at a current of 20 mA g<sup>-1</sup>, at a C/15 rate, from 1 M solution of Mg(ClO<sub>4</sub>)<sub>2</sub> in acetonitrile. (b) Cyclic voltammetric reversible scan of nanostructured V<sub>2</sub>O<sub>5</sub> developed on CNF (shown in blue) and a CNF capacitive scan taken in 1 M Mg(ClO<sub>4</sub>)<sub>2</sub> dissolved in acetonitrile at a scanning rate 0.02 mC s<sup>-1</sup>. (c) Enhanced specific capacity and stability of the electrode measured for 50 cycles. (d) Differential capacity (dQ/dV) plot (of corresponding third charge–discharge cycles of same cathode at the C/10 rate) exhibiting two distinctive reversible primary peaks in the range 0–2 V for a V<sub>2</sub>O<sub>5</sub>/Sn full cell. (e) Curves indicating the 20th and 50th charge–discharge cycle. There are noticeable increases in the capacity for the 50th cycle. Reprinted with permission from ref 71. Copyright 2015 American Chemical Society.

nanowires reached 130 mAh g<sup>-1</sup> in the sixth cycle at C/20. The structural development and reversibility of Mg insertion/extraction were observed by operando synchrotron diffraction and X-ray absorption spectroscopy during cycling.<sup>73</sup> After that, under the supervision of Malachi Noked, the hierarchical design and synthesis of monodispersed spherical V<sub>2</sub>O<sub>5</sub> resulted in a discharge capacity that decreased from an initial value of 225 mAh g<sup>-1</sup> to 190 mAh g<sup>-1</sup> at 10 mA g<sup>-1</sup>. After being put through 100 cycles, the V<sub>2</sub>O<sub>5</sub> spheres still had a Coulombic efficiency of 95% and possessed a specific discharge capacity of 55 mAh g<sup>-1</sup> when operating at a moderate current rate of 50 mA g<sup>-1</sup>. This capacity reduced by only 5% and 13% after 50 and 100 cycles, respectively. Even after repetitive intercalation–deintercalation at varied current rates, the exact phase and morphology remained identical, demonstrating excellent stability during Mg<sup>2+</sup> ion intercalation–deintercalation.<sup>74</sup> Despite having a relatively low salt content of 0.8 molal (m) magnesium(II) bis(trifluoromethanesulfonyl)imide Mg(TFSI)<sub>2</sub>, in a recent study, it was demonstrated that an electrochemical stability window of 3.7 V can be maintained in aqueous magnesium-ion electrolytes (AMEs). Molecular

crowding agent PEG 400 (polyethylene glycol) affects electrochemical/physicochemical features of the AME and suppresses water splitting. Capacity retention at 50 mA g<sup>-1</sup> is 80% after 100 cycles for V<sub>2</sub>O<sub>5</sub> nanowires in the 0.8 m Mg(TFSI)<sub>2</sub>/85% PEG/15% H<sub>2</sub>O (AME), which translated to a discharge capacity of 286 mAh g<sup>-1</sup>. An Mg-rich Mg<sub>x</sub>V<sub>2</sub>O<sub>5</sub> (x ≈ 1.0) phase was detected by XRD for the first time. The first evidence that the cathode electrolyte interface can form and break down in MIBs reversibly is presented here. Sustainable large-scale energy storage was made possible by the methodology shown, which involved the design of high-performance cathode materials and environmentally benign, high-safety, high-voltage, and cheap aqueous electrolytes.<sup>75</sup>

Under the supervision of Seung-Tae Hong, MIBs have found a high-energy cathode material in H<sub>2</sub>V<sub>3</sub>O<sub>8</sub>. The average discharge voltage is 1.9 V vs Mg/Mg<sup>2+</sup>, and the initial discharge capacity is 231 mAh g<sup>-1</sup> at 60 °C, indicating reversible magnetization–demagnetization activity. The first ever determination of the crystal structure of Mg<sub>0.97</sub>H<sub>2</sub>V<sub>3</sub>O<sub>8</sub> reveals an easily accessible channel for Mg-ions to move throughout the material. The material's exceptional performance was due

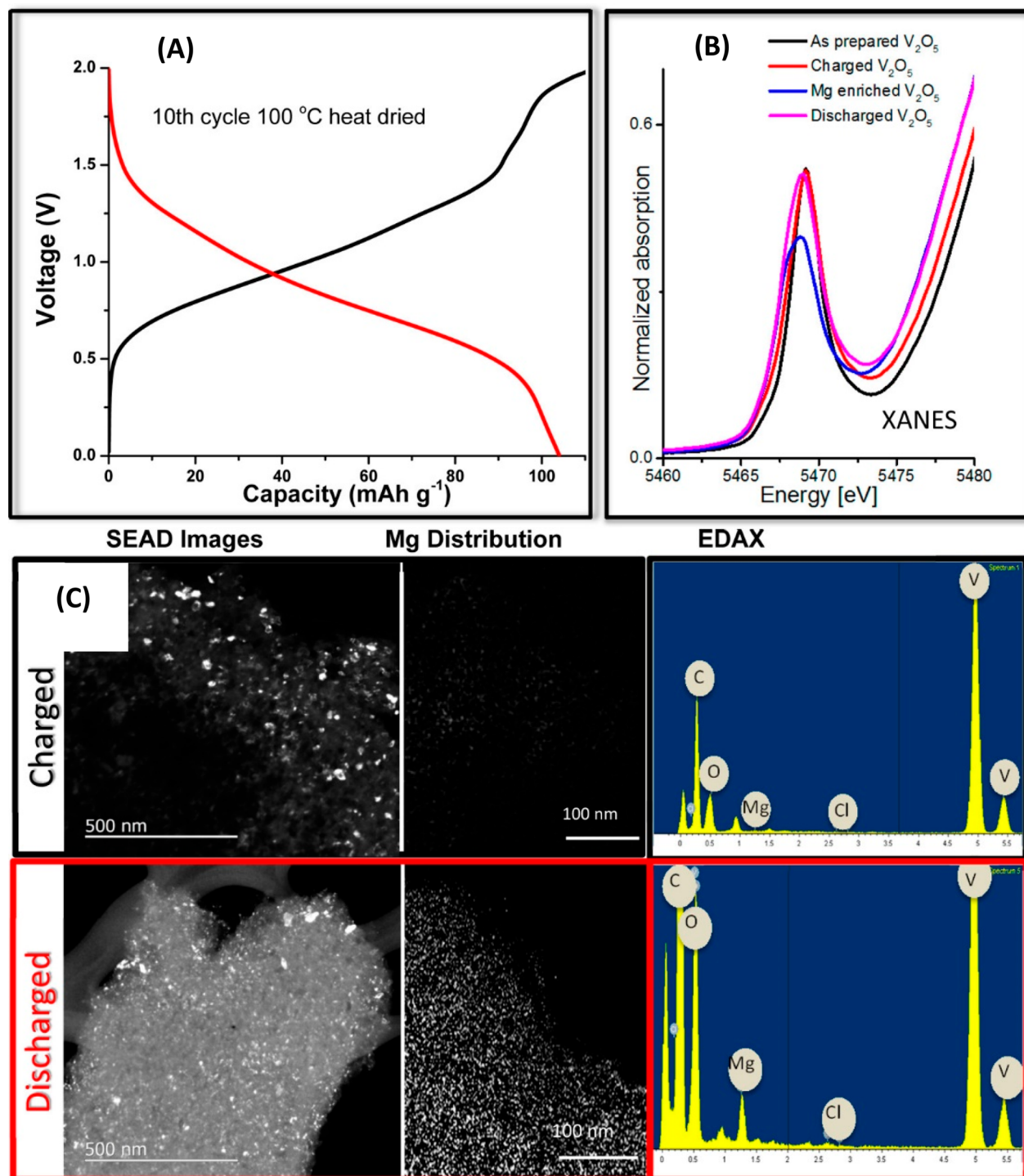


**Figure 5.** (a) Charge–discharge graph of Mg-supplemented bilayered  $V_2O_5$  against a nanocrystalline Sn anode taken after the tenth cycle within the potential window of 2.0–0.0 V (against  $Mg/Mg^{2+}$ ), cycled at current rate of 20 mA  $g^{-1}$  from a 1 M solution of  $Mg(ClO_4)_2$  in acetonitrile. (b) Normalized K-edge XANES spectra of Mg-supplemented, charged–discharged (taken after 10th cycle), and as-prepared bilayered  $V_2O_5$  against a Sn anode in a full cell. (c) Selected area electron diffraction (SAED) images in the presence and absence of magnesium (left and center) during different states of charging concurrent with elemental analysis obtained using an energy dispersive X-ray analysis (EDAX) detector in TEM. Reprinted with permission from ref 71 Copyright 2015 American Chemical Society.

to its unique crystal structure, which makes use of hydrogen bonding as well as water–metal bonding to provide a high energy density of 440  $Whkg^{-1}$ , making it an excellent candidate for novel high-energy materials and oxide-based stable materials for MIBs.<sup>76</sup> Ji et al. investigated that Vanadium pentoxide  $VOPO_4$ , after being treated with water, has been

offered as an alternative cathode material for MIBs. The electrochemical studies have shown that the cathode of  $VOPO_4$  is activated by both water present in the material and water in the organic electrolyte. Water in an aqueous electrolyte exists in thermodynamic equilibrium with the water molecules in the  $VOPO_4$  lattice, highlighting the mechanism



and kinetics for Mg-ion insertion. In the presence of water, both the diffusion barrier within a solid and the desolvation penalty at the interface were reduced to a lower level. In order to achieve rapid reaction kinetics, an electrolyte with a water activity of  $>10^{-2}$  was necessary. The suggested activation mechanism facilitated the development of high-performance multivalent-ion batteries.<sup>77</sup>

In one particular study under the supervision of Seung-Tae Hong, a high-performance cathode material for MIBs,  $\text{NH}_4\text{V}_4\text{O}_{10}$ , was synthesized to display reversible magnetization by using acetonitrile and 0.5 M  $\text{Mg}(\text{ClO}_4)_2$  as the electrolyte. It has an initial discharge capacity of  $174.8 \text{ mAh g}^{-1}$  and an average discharge voltage of 2.13 V (against  $\text{Mg}/\text{Mg}^{2+}$ ). An organic electrolyte with a somewhat high water concentration was used for the first time to show that electrochemical magnetization may be performed at a voltage greater than 2 V (against  $\text{Mg}/\text{Mg}^{2+}$ ).<sup>78</sup>  $\text{Mg}_3\text{V}_2\text{O}_8$  (MVO) was investigated for its potential use as a cathode material for MIBs due to its high rate and cycle performance. Two-phase and single-phase solid solution reactions were linked to the  $\text{Mg}^{2+}$  storage mechanism. Zuo et al. reported a complete Mg cell with an MVO cathode and a titanium–niobium oxide (NTO) anode in a standard electrolyte, which showed a reversible capacity of  $102 \text{ mAh g}^{-1}$ . This study showed a promising Mg-extractable cathode material that is compatible with common electrolytes. It also created novel possibilities for research into magnesium cathode materials.<sup>79</sup>

In a recent study, Ma et al. showed that the calcination of  $\text{Mg}_3\text{V}_2\text{O}_8$  (MVO) at high temperatures in  $\text{Mg}^{2+}$  electrolyte solution is helpful for reducing the price of aqueous Mg-ion batteries. MVO demonstrated strong electrochemical rate capability with a reversible discharge specific capacity of  $143 \text{ mAh g}^{-1}$  at the current density of  $0.05 \text{ Ag}^{1-}$  and that of  $61 \text{ mAh g}^{-1}$  at  $4 \text{ Ag}^{1-}$ , as well as good cyclic performance with 81% capacity after 1000 cycles at  $3 \text{ Ag}^{1-}$ . These results revealed that MVO is a good option for MIBs.<sup>80</sup> In a recent scientific effort, due to the high specific capacity of  $262 \text{ mAh g}^{-1}$ , ultralong cycle life, and high rate capability of  $\text{Cu}_3\text{V}_2\text{O}_7 \cdot 2\text{H}_2\text{O}$  (CVOH), it is demonstrated as a superior Mg-hosting cathode. To maximize performance, lamellar-structured  $\text{V}_6\text{O}_{13}$  nucleates in superficial CVOH during discharging and interweaves with CVOH layers to build a Mg-ion diffusion highway on the CVOH surface. By further stabilizing the CVOH structure through interweaving, an extremely extended cycle life was achieved. This mechanism presented an innovative approach to the creation of high-performance electrodes for multivalent-ion batteries.<sup>81</sup> Doping was also done in the case of oxides of vanadium to get enhanced properties. Therefore, sulfur-doped vanadium pentoxide ( $\text{S}-\text{V}_2\text{O}_5$ ) has a specific capacity of  $300 \text{ mAh g}^{-1}$  and could be utilized as a cathode material for MIBs. A low-temperature plasma of carbon felt and a 2.5 GHz microwave generator produced  $\text{S}-\text{V}_2\text{O}_5$ . This study investigated the high capacity of  $\text{S}-\text{V}_2\text{O}_5$  in metal oxides.  $\text{MnO}_2$  added to composite  $\text{SMn}-\text{V}_2\text{O}_5$  which contains more sulfur than  $\text{S}-\text{V}_2\text{O}_5$ , produced the maximum capacity ( $420 \text{ mAh g}^{-1}$ ).<sup>82</sup>

There are numerous cathode materials for MIBs based on vanadium and its oxides. Each of these compounds can be utilized according to their specific properties. Bilayered  $\text{V}_2\text{O}_5$  displayed excellent discharge capacity, while monodispersed  $\text{V}_2\text{O}_5$  spheres showed remarkable capacity retention along with other electrochemical properties. Moreover, a recent study has shown that majority of oxides do not intercalate except Mg-

ion, other than  $\text{V}_2\text{O}_5$ , while the conversion reaction is observed in case of other oxides.<sup>83</sup> Figures 4 and 5 illustrate the electrochemical performance of nanostructured bilayered  $\text{V}_2\text{O}_5$  as a cathode material for MIBs.

**3.5. Sulfur-Based Cathode Materials.** Kravchyk et al. determined that the nanostructured CuS cathode material displayed highly reversible insertion of Mg-ions and had a specific capacity of  $300 \text{ mAh g}^{-1}$ . It also demonstrated good cyclic stability over 200 cycles at a current density of  $0.1 \text{ Ag}^{1-}$  and had a Coulombic efficiency of 99.9%. The utilization of nanostructuring resulted in an improvement in the kinetics of conversion reactions, outperforming bulk CuS, which is only active at a temperature of  $50 \text{ }^\circ\text{C}$ .<sup>84</sup> Later, Le and co-workers utilized hydrothermal treatment to create  $\text{Cu}_2\text{MoS}_4$  nanotubes with a large square cross-section of  $100\text{--}170 \text{ nm}$ . These nanotubes have shown a discharge capacity of up to  $390 \text{ mAh g}^{-1}$ , which indicated that they have the potential to be used as a high-energy-capacity cathode for MIBs. This study underlined the effect that crystal structure and particle morphology had on electrochemical parameters, and it offered some useful insights for improving electrode performance in MIBs.<sup>85</sup>

Recently, Shen et al. developed a CuS-CTAB-2 (CTAB = cetyltrimethylammonium bromide) electrode, which proved to be a high-energy cathode material for MIBs that had a noncorrosive Mg-ion electrolyte. With a reversible capacity of  $477 \text{ mAh g}^{-1}$  and remarkable energy densities of  $415 \text{ Wh kg}^{-1}$  and  $1909 \text{ Wh L}^{-1}$ , it provided outstanding extended cycling stability over 1000 cycles. The specific surface area of CuS was increased by the incorporation of CTAB due to the expansion of its interlayers and improvement of its shape. The technique proved to be effective in the design of high-performance cathode materials based on metals that can be used in MIBs that have a suitable electrolyte.<sup>86</sup> After that, Fei Xu and her lab fellows demonstrated the superior performance of ammonium tetrathiomolybdate as an MIB cathode. At  $50 \text{ mA g}^{-1}$ , ammonium tetrathiomolybdate displayed a high capacity of  $333 \text{ mAh g}^{-1}$ , and at  $5.0 \text{ Ag}^{1-}$  it demonstrated a decent rate performance of  $129 \text{ mAh g}^{-1}$ . During the first cycle, ammonium is taken out to make an amorphous structure with many active sites for storing magnesium and open paths for its motion. Because the negative charge is not concentrated in one area, the covalent-like bond between molybdenum and sulfur reduces the interaction with the bivalent magnesium cation and speeds up the kinetics. The covalent-like molybdenum–sulfur bond is what is responsible for the high specific capacity, as it makes it possible for molybdenum and sulfur to undergo redox reactions at the same time. This work presented a new high-capacity and high-power MIB cathode material, explained the mechanism behind its exceptional performance, and offered guidance for improving the design and efficiency of MIB cathode materials.<sup>87</sup> In the past, ultrasmall Mg nanoparticles with an average diameter of  $2.5 \text{ nm}$  and extensively exfoliated graphene-like  $\text{MoS}_2$  ( $\text{G}-\text{MoS}_2$ ) NPs had been synthesized. With a high working voltage of 1.8 V and a first discharge capacity of  $170 \text{ mAh g}^{-1}$  that stayed at 95% after 50 discharge–charge cycles, the combination of  $\text{G}-\text{MoS}_2$  as the cathode and Mg as the anode was proven to be one of the most successful combinations for rechargeable magnesium batteries. Thus, this result provided new paths for enhancing the electrochemical functionality of MIBs.<sup>88</sup>

All the S-based cathode materials showed enhanced characteristics compared to the other reported cathode materials. Among S-based materials, CuS-CTAB-2 showed

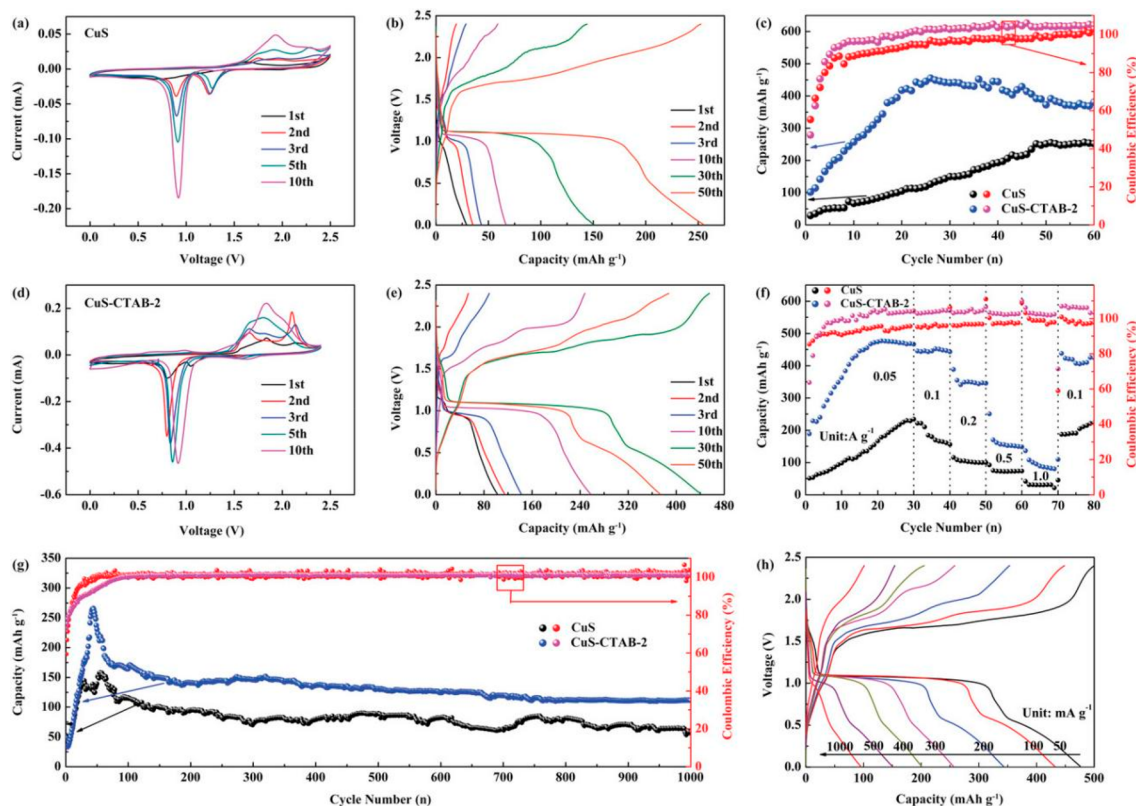


**Figure 6.** Cyclic voltammetric curves of as-prepared (a) CuS and (d) CuS-CTAB-2 electrodes in a voltage range of 0.01–2.24 V at a 0.1 mV s<sup>-1</sup> scan rate. Galvanostatic charge and discharge (GCD, current density of 100 mA g<sup>-1</sup>) profiles of (b) CuS and (e) CuS-CTAB-2 cathodes. Long-term cycling performance at high current densities of (c) 100 and (g) 560 mA g<sup>-1</sup>. (f) High reversible discharge capacities at current densities ranging from 50 to 1000 mA g<sup>-1</sup>. (h) GCD profiles showing reversible discharge capacities of the CuS-CTAB-2 cathode at varying current densities. Reprinted with permission from ref 86. Copyright 2020 John Wiley and Sons.

remarkable discharge capacity, energy density, and excellent cycle life. Figure 6 represents the CV curves, charge and discharge profiles, and other electrochemical properties of CuS and CuS-CTAB-2.

**3.6. Mg<sup>2+</sup>-Containing Cathode Materials.** Honma and his team synthesized olivine-type MgMnSiO<sub>4</sub> and MgCoSiO<sub>4</sub> nanoparticles at low temperatures using fast superficial fluid processing. The reduced electrochemical resistance was a result of the small crystalline size and short Mg diffusion length. Both nanoparticles showed discharge capacities of 70.5 and 88.0 mAh g<sup>-1</sup>, respectively, when utilized as a cathode in MIBs.<sup>89</sup> Later, olivine-structured magnesium ferrous silicate (MgFe-SiO<sub>4</sub>) for magnesium batteries showed crucial atomic-scale insights. Doping on the Si sites with trivalent atoms such as Al, Ga, or V is undesired; however, doping on the Fe sites with the Mn or Co was expected to enhance the cell voltage more than 2.70 V. However, the voltage went beyond the region of electrochemical stability upon Ni doping. The research revealed useful information for improving silicate base electrodes in MIBs in the future.<sup>90</sup> Silicate-based Mg-ion cathodes have been critically doubted by the scientific community because of their low energy density and poor cycling stability. The silicate-based cathodes have a lower energy density than other cathode materials, which means that they can store less energy per unit mass or volume. Additionally, the cycling stability of these cathodes is poor, meaning that they degrade quickly over time and lose their ability to store energy. However, it is important to note that research in this area is ongoing, and new developments may

lead to improvements in the performance of silicate-based Mg-ion cathodes in the future.<sup>91</sup>

Under the supervision of a former scientist, MgMn<sub>2</sub>O<sub>4</sub>, with a theoretical capacity of 272 mAh g<sup>-1</sup>, proved to be a promising cathode material for high volumetric MIBs. Atomic-resolution imaging using aberration-corrected scanning transmission electron microscopy (STEM) revealed the atomic structure of cubic spinel MgMn<sub>2</sub>O<sub>4</sub> and the formation of a thin and stable surface layer of rock salt MgMnO<sub>2</sub>. After Mg was injected into the spinel lattice, Frenkel defect-mediated Mg cation repositioning and Mg/Mn cation exchange provoked this formation. Structural studies emphasized spinel oxide's electrochemical performance in MIBs.<sup>92</sup> Kobayashi et al. synthesized cubic Mg–Mn spinel oxide nanoparticles approximately 5 nm in size through the reduction of alcohol at room temperature. The Mg(ClO<sub>4</sub>)<sub>2</sub>/CH<sub>3</sub>CN electrolyte composite, which was coated with graphene to prevent aggregation, exhibited a specific capacity of 230 mAh g<sup>-1</sup> and was capable of being cycled more than 100 times without experiencing a significant loss in capacity, even when subjected to moderate current density.<sup>93</sup> In a recent study, Mg<sup>2+</sup> was utilized at high Mn redox potentials in a customized solid solution spinel called MgCrMnO<sub>4</sub>, with bulk Mg<sup>2+</sup> deintercalation facilitated by electrostatic contact between Mg<sup>2+</sup> and O<sup>2-</sup>. The Mg/Mn antisite version can be reduced to less than 10% with postannealing treatment at 350 °C, which also helped improve the mobility of Mg<sup>2+</sup>. It was found that it is possible to harvest up to about 180 Wh kg<sup>-1</sup> of spinel at a temperature of 60 °C when it is in charged condition at a high potential of about 3.0

V (versus Mg/Mg<sup>2+</sup>). This observation paved the way for the construction of a realistic high-voltage Mg-ion cathode by making use of spinel oxide.<sup>94</sup> Zhu, with his lab fellows, used sol–gel synthesis to create MgFe<sub>x</sub>Mn<sub>2-x</sub>O<sub>4</sub> nanomaterials ( $x = 0.67, 1.33, 1.6$ ) with the molar ratio of iron to manganese controlled by the  $x$  value to increase electrochemical performance at a low cost. The modified MgFe<sub>1.33</sub>Mn<sub>0.67</sub>O<sub>4</sub> showed good cycling performance and rate capability, having a specific capacity of 88.3 mAh g<sup>-1</sup> after 100 cycles despite having a high current density of 1000 mA g<sup>-1</sup>. The structure of MgFe<sub>1.33</sub>Mn<sub>1.67</sub>O<sub>4</sub> was found to be stable and showed potential for cycling stability. Furthermore, it was also revealed that oxygen and hydrogen evolution during charging–discharging could be successfully inhibited by adjusting the atomic ratio in the compound. The increased magnesium diffusion coefficient at two oxidation peaks significantly boosted the rate capability.<sup>95</sup>

Similarly, a reductive solvothermal technique was used to synthesize nanosized MgMn<sub>2</sub>O<sub>4</sub> (MMO) spinel at a temperature of less than 200 °C. In addition, a composite of MMO and CNT was developed, which showed increased discharge capacity in comparison to the MMO cathode. The enhancement in capacity was contributed to the increase in the number of redox-active MMOs and electrical double-layer capacitance. This straightforward solvothermal method contributed to the expedient synthesis of more spinel nanoparticles for possible application as high-voltage cathodes in MIBs.<sup>96</sup> Asif et al. accomplished the synthesis of SnO<sub>2</sub>-rGO composites through the application of electrostatic contact by maintaining the temperature at a low level. The composites were tested for usage as electrode components in magnesium and magnesium/lithium hybrid ion batteries. The optimum specific capacity of the MIB's cell was determined to be 222 mAh g<sup>-1</sup> when it was subjected to 20 mA g<sup>-1</sup>, and the cells maintained 90.05% of their initial power. At the same current density, the magnesium/lithium-ion battery's maximum capacity was 350 mAh g<sup>-1</sup>, but its capacity retention was lower than expected due to the volume expansion of the SnO<sub>2</sub> NPs. According to the results of the research, tin oxide that has been embedded in rGO is a promising choice for risk-free and high-performance MIB cathodes.<sup>97</sup> Similar to the above study, the MgMn<sub>2</sub>O<sub>4</sub>/rGO composite showed an initial capacity of 305 mA g<sup>-1</sup> and almost no capacity loss after 100 cycles, while the MgMn<sub>2</sub>O<sub>4</sub> composite sample had an initial capacity of 120 mA g<sup>-1</sup> and lost about 25% of its initial capacitance after the same number of charges and discharges. The performance of the composite sample was enhanced in terms of both its capacity retention and reversibility with the addition of rGO. The redox mechanism and electrochemical mechanism at both electrodes were very comparable. Studies of electrochemical impedance demonstrated that, after surface modification by rGO, the composite sample had much lower charge transfer resistance, indicating better electrical conductivity between the active substance and electrolyte at the interface.<sup>98</sup>

Hatakeyama et al. comprehensively studied different polymorphs of MnO<sub>2</sub> ( $\alpha$ -MnO<sub>2</sub>,  $\beta$ -MnO<sub>2</sub>,  $\gamma$ -MnO<sub>2</sub>,  $\delta$ -MnO<sub>2</sub>, and  $\lambda$ -MnO<sub>2</sub>). Among these, the intercalation of Mg into  $\alpha$ -MnO<sub>2</sub> results a remarkable capacity range of 150–220 mAh g<sup>-1</sup> while avoiding the formation of rock salt or spinel phases. This intercalation capacity remains consistent even at a discharge capacity of 270 mAh g<sup>-1</sup>. In contrast, Mg insertion into  $\beta$ -MnO<sub>2</sub> eventually produces a transformation.  $\delta$ - and  $\lambda$ -MnO<sub>2</sub> thermally degraded into Mn<sub>3</sub>O<sub>4</sub> at a temperature of 150

°C, suggesting the low structural stability of MnO<sub>2</sub> polymorphs. Experimental results demonstrated that the process of Mg intercalation in  $\alpha$ -MnO<sub>2</sub> exhibits greater stability and faster kinetics compared to the  $\alpha$ -type structure conversions, while  $\beta$ -MnO<sub>2</sub> was highly stable.<sup>99</sup> Figure 7

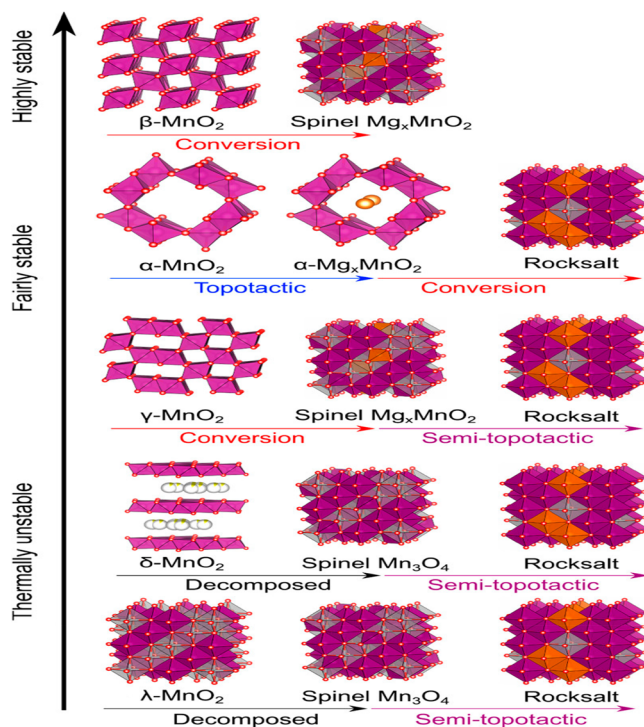


**Figure 7.** A schematic representation is presented depicting the ergodic pathways associated with the Mg-induced phase change of MnO<sub>2</sub> polymorphs. These pathways have been observed experimentally by electrochemical tests conducted at a temperature of 150 °C. Reprinted with permission from ref 99. Copyright 2021 American Chemical Society.

presents the pictorial illustration of the Mg-induced phase change of MnO<sub>2</sub> polymorphs. A few years ago, Okamoto et al. studied different spinel and rock salt structures (MgCo<sub>2</sub>O<sub>4</sub>, MgMn<sub>2</sub>O<sub>4</sub>, MgFe<sub>2</sub>O<sub>4</sub>, MgCr<sub>2</sub>O<sub>4</sub>, and Co<sub>3</sub>O<sub>4</sub>) as cathode materials for MIBs. The process of Mg insertion in the spinel structure of MgCo<sub>2</sub>O<sub>4</sub> occurs at a voltage of 2.9 V relative to that of the Mg<sup>2+</sup>/Mg reference electrode. The experimental results were in accordance with ab initio calculations. The capacity of this Mg insertion process is measured to be 200 mAh g<sup>-1</sup>, whereas the theoretical capacity is estimated to be 260 mAh g<sup>-1</sup>. The demagnetization of MgMn<sub>2</sub>O<sub>4</sub> and MgCr<sub>2</sub>O<sub>4</sub> can be achieved by utilizing the Mg insertion/extraction potential, which has a value of 3.4 V relative to the Mg<sup>2+</sup>/Mg reference electrode. The “intercalation and push out” technique is believed to have the potential to generate polyvalent cation cathode materials, which will be helpful in future rechargeable batteries.<sup>100</sup>

Among numerous Mg<sup>2+</sup>-containing cathode materials, the materials containing rGO showed good electrochemical properties. The other materials can be utilized as cathode materials, but they were not strong enough to show excellent capacity retention and enhanced electrochemical properties. Table 2 shows the comparison of different cathode materials that are discussed. The comparison is between the discharge capacity (mAh g<sup>-1</sup>), capacity retention, cycle life, and current

Table 2. Comparison of Various Nanostructure-Based Cathode Materials for MIBs

s. no.	cathode materials	discharge capacity (mAh g <sup>-1</sup> )	electrolyte	capacity retention	cycle life	current density (mA g <sup>-1</sup> )	refs
1	Hol MnO <sub>2</sub> /AB	210	Mg(ClO <sub>4</sub> )			100	60
2	MnO <sub>2</sub> /CNTs	92		75	35		62
3	birnessite MnO <sub>2</sub>	231.1	MgSO <sub>4</sub>	62.5	1000		63
4	Ni <sub>3</sub> Se <sub>4</sub>	99.8	APC/THF	75	100		65
5	WSe <sub>2</sub> nanosheet	>265	APC second generation			50	66
6	1T-VSe <sub>2</sub> @rGO	235.5	APC	62.7	500	50	67
7	CuSe	357	ether-based Mg-ion electrolyte			100	68
8	β-Cu <sub>2</sub> Se	230	Mg[N(CF <sub>3</sub> SO <sub>2</sub> ) <sub>2</sub> ] <sub>2</sub> /acetonitrile				69
9	VO <sub>x</sub> nanotubes	>200	Mg(ClO <sub>4</sub> ) <sub>2</sub> in deaerated acetonitrile				70
10	bilayered V <sub>2</sub> O <sub>5</sub>	240					71
11	V <sub>2</sub> O <sub>5</sub> /GNP	90	MgNO <sub>3</sub> ·6H <sub>2</sub> O, succinonitrile, tetraethylene glycol, dimethyl ether				72
b12	orthorhombic V <sub>2</sub> O <sub>5</sub> nanowires	130	Mg(ClO <sub>4</sub> ) <sub>2</sub>				73
13	monodispersed V <sub>2</sub> O <sub>5</sub> spheres	190	LP57	95	100	10	74
14	H <sub>2</sub> V <sub>3</sub> O <sub>8</sub>	231	Mg(ClO <sub>4</sub> ) <sub>2</sub> in acetonitrile				76
15	Mg <sub>3</sub> V <sub>2</sub> O <sub>8</sub>	102	Mg(TFSI) <sub>2</sub> in acetonitrile		1000		79
16	CVOH	143	MgCl <sub>2</sub>			50	81
17	CuS	300			200		84
18	Cu-CTAB-2	477	Mg[B(hfp) <sub>4</sub> ] <sub>2</sub> /DME		1000		86
19	MgFe <sub>1.33</sub> Mn <sub>0.67</sub> O <sub>4</sub>	88.3	MgCl <sub>2</sub>		100	1000	95
20	SnO <sub>2</sub> -rGO	222	APC	90.05		20	97
21	MgMn <sub>2</sub> O <sub>4</sub> /rGO	305	MgSO <sub>4</sub> in 1:10 water/acetonitrile		100		98

density (mA g<sup>-1</sup>). Figure 8 displays the graph between the cathode materials on the abscissa and discharge capacity on the

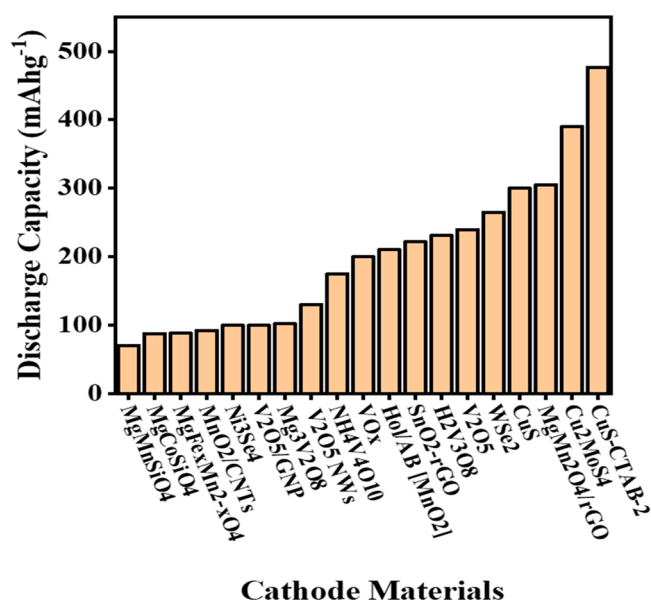


Figure 8. Bar graph of various cathode materials based on their increasing discharge capacity.

ordinate. The graph is based on increasing the discharge capacity of cathode materials.

#### 4. DENSITY FUNCTIONAL THEORY STUDIES OF THE CATHODE MATERIALS

In quantum mechanics, the computational method known as density functional theory (DFT) is used to study and predict the behavior of electrons in atoms, molecules, and solids.<sup>101</sup>

Molecular geometry, energy, and reaction routes are just some of the many aspects that may be determined with DFT by focusing on the electron density and how it relates to the external potential.<sup>102</sup> The study of inaccessible systems and the development of new materials are aided by this technology. Although it has its limitations, DFT is a cost-effective alternative to complex experiments.<sup>103</sup> However, DFT is still an effective method for understanding and forecasting the behavior of atoms and molecules.<sup>104</sup> Cathode materials for MIBs can be studied via DFT to investigate their many properties. The density of states, electrical band structures, and crystal structures can all be predicted with this method. Calculations using the DFT method can be used to determine voltage profiles, evaluate diffusion properties, and predict the reaction energy. Flaws and interfaces of cathode materials can also be explored with DFT. Researchers can get insights into the performance and behavior of the cathode material by utilizing DFT. These insights may then be used to direct the development of cathode materials for MIBs that are more efficient and stable.<sup>105–107</sup>

Discrepancies between theoretical predictions derived from DFT and practical results frequently arise due to intrinsic approximations within DFT, including the selection of certain parameters or functional forms.<sup>108</sup> The disparities can be attributed to factors such as system complexity, fluctuations in temperature and pressure, and the difficulties encountered in accurately modeling dispersion interactions.<sup>109</sup> The presence of inherent constraints in DFT, such as the omission of specific electronic correlation effects and dynamic effects, can also exert an influence. The observed inequalities are further influenced by the structural variations between theoretical models and experimental settings, as well as the challenge of appropriately considering solvent effects.<sup>110</sup> To resolve these discrepancies, it is necessary to refine theoretical approaches, consider addi-

tional factors, and acknowledge the inherent limitations of both theoretical and experimental methods.<sup>111</sup>

First-principles DFT computations of the WSe<sub>2</sub> were carried out so that an analysis of the influence of Mg-intercalation behavior could be performed. The findings of the study indicated that these batteries may have applications in the optoelectronics systems of the upcoming generation.<sup>64</sup> Later, two distinct types of molybdenum chalcogenide halide nanowires were studied to be utilized as potential cathode materials for MIBs. It was discovered through the use of density functional theory calculations that pure selenium-based nanowires had the most exothermic Mg adsorption energies. Furthermore, it was observed that Mo<sub>6</sub>Se<sub>6</sub> nanowires have the potential to have low Mg diffusion barriers and high specific capacities. The performance of these nanowires was evaluated in this work, and it was compared to that of other contemporary cathode materials.<sup>112</sup> Pan and his team suggested that Mg<sub>x</sub>FePO<sub>4</sub> is a material that can be utilized as a cathode for MIBs, and it is capable of achieving a reversible capacity of 82 mAh g<sup>-1</sup>. Calculations based on the “first-principles” revealed that the capacity of the cathode is limited by strong Mg-ion interactions, which in turn lead to asymmetric discharge and charge behavior. This work explained how Mg-ions intercalate and deintercalate in FePO<sub>4</sub> and can be utilized as a reference when developing cathode materials for multivalent metal-ion batteries.<sup>113</sup>

Shasha et al. utilized computational and experimental methods to investigate whether Mg ions could be removed electrochemically from the MgNiMnO<sub>4</sub> material. Mg ion diffusion was found to be energetically unfavorable when the DFT+U method was employed to model its motion in the MgNiMnO<sub>4</sub> unit cell. The lack of activation observed in electrochemical experiments further demonstrated that Mg ion migration is impossible in MgNiMnO<sub>4</sub>.<sup>114</sup> Kulik investigated whether DFT+U can be used to represent the localized 3d or 4f orbitals contained in the elongated s–p states found in many strongly correlated materials and perovskites due to its applicability to all open-shell orbitals, including d and f orbitals for transition metal elements.<sup>115</sup> Under the supervision of Lee, Mg<sub>3</sub>Si<sub>3</sub>(MoO<sub>6</sub>)<sub>2</sub> proved to be a suitable cathode material for high-performance MIBs because of its high discharge voltage (2.35 V against Mg/Mg<sup>2+</sup>), low ion migration barrier of 0.2 eV, and small volume change of up to 4%. Due to these properties, it was an excellent candidate to be used in cathodes. First-principles calculations revealed a new path toward the construction of effective MIBs for future energy storage, linking the low energy barrier for ion migration to favorable changes in Mg coordination inside the garnet host.<sup>116</sup>

According to DFT-based first-principles calculations, the Mg atoms exhibited metallic properties and high electronic conductivity by strongly binding with VS<sub>2</sub>. The highest theoretical capacity for MIBs is 233 mAh g<sup>-1</sup>, and this is true for all three types of VS<sub>2</sub>, that is, monolayer VS<sub>2</sub> (M-VS<sub>2</sub>), double-layer VS<sub>2</sub> (D-VS<sub>2</sub>), and bulk VS<sub>2</sub> (B-VS<sub>2</sub>). In MIBs, M-VS<sub>2</sub> with its excellent rate performance can serve as an anode material thanks to the low diffusion barriers of Mg, while D-VS<sub>2</sub> and B-VS<sub>2</sub> can serve as cathode materials depending on the typical operating voltages.<sup>105</sup> Ahmad and co-workers found that a benzoquinone-based microporous conjugated polymer (BQMCP) can be a viable cathode material for MIBs in DFT simulations. Simulations showed that BQMCP has a high binding energy for Mg<sup>2+</sup> ions, with a theoretical capacity of

467.038 mAh g<sup>-1</sup> and a maximum storage capacity of up to 12 Mg ions. With positive redox potential values of 2.58 and 2.45 V for one and two Mg ions, respectively, BQMCP showed potential as a cathode material for MIBs, with the capacity to accommodate more Mg-ions than previously reported. The results of this study suggested that BQMCP could be employed in real-world applications in the future, which would result in the development of MIBs with a high energy density suitable for large-scale.<sup>117</sup>

Yang et al. explored the potential cathode materials for MIBs, including MoO<sub>2</sub> and two types of MoOSe, using first-principles calculations. Theoretical capacities of 279, 191, and 191 mAh g<sup>-1</sup> were observed for Mg cations intercalated into octahedral sites in MoO<sub>2</sub> and the two types of MoOSe, respectively. The cathode materials for Mg-ion batteries showed promise, with anticipated plateaus of discharge around 1 V. The authors also showed that the volume increased and diffusion barriers formed during the Mg intercalation process. The results suggested layered MoO<sub>2</sub> and MoOSe could be excellent options for MIBs cathode materials.<sup>118</sup> Sivaraman and his co-workers carried out first-principles DFT computations and evaluated the application of a graphene-like boron nitride (G-BN<sub>nyen</sub>) monolayer in MIBs. Mg storage was consistent, with adsorption energies from -1.94 to -0.59 eV. Ion diffusion barriers were 0.27–0.12 eV. The theoretical capacity was 939.16 mAh g<sup>-1</sup>, showing better efficiency than previously examined cathodes. The optimal cell voltage window and low migration energies suggested that Mg-based MIBs can charge quickly.<sup>119</sup>

In a most recent study, Khan et al. used computational simulations to accelerate the hunt for next-generation energy sources like MIBs by proposing a new cathode materials for MIBs: a porous polymer-based quinone-functionalized hexahydroxytriphenylene (QHHTP) and diphenylbutadienynebis-(boronic acid) (DPB). The material has substantial Mg ion affinities for quinone ring C=O sites that are stable and porous. The polymer layer unit can be fully loaded with Mg ions at various active sites, and QHHTP-DPB has a specific theoretical capacity of 720.48 mAh g<sup>-1</sup> and a positive low open circuit voltage of 0.39 V. MIBs had higher cycling performance and high capacity because QHHTP-DPB has no structural change and the HOMO–LUMO gap decreases more after Mg-ions adsorb onto the polymer. This quinone-functionalized HHTP-DPB porous polymer could be future MIB cathode material.<sup>120</sup>

## 5. CONCLUSION

Undoubtedly, energy is a prime need of human beings. Because of the toxic effects and constraints of nonrenewable energy sources, the world is focusing on renewable energy sources. Solar and wind energy are being produced consistently, but there is unpredictability in the amount of energy that is being generated. Therefore, there is a potential need for ESSs. Among different types of ESSs, batteries are proven to be prominent energy storage devices. LIBs have prompted a wide range of applications; however, the performance indexes of LIBs are reaching their limits. Among many types of batteries available, MIBs stand out due to their many advantageous features; however, the cathode materials for MIBs are limiting their performance. To increase the capacity and energy density of current cathodes, it is essential to be aware of the reported cathode materials and their characteristics.

Cathode materials for Mg-ion-based batteries include Mn-based, Se-based, vanadium- and vanadium oxide-based, S-based, and Mg<sup>2+</sup>-containing cathode materials. HoI/AB showed a high discharge capacity, while  $\alpha$ -MnO<sub>2</sub> showed a high reversible capacity. Mn<sub>3</sub>O<sub>4</sub> nanoparticles, due to their large surface area, showed high Coulombic efficiency. The MnO<sub>2</sub>/CNTs showed a good specific capacity and retained a capacity of 75%. Among Se-based cathode materials, WSe<sub>2</sub> nanosheets showed a high discharge capacity and notable rate capability as compared to the WSe<sub>2</sub> nanowire film. Among V- and VO<sub>x</sub>-based cathode materials, layered V<sub>2</sub>O<sub>5</sub> showed an excellent discharge capacity, followed by H<sub>2</sub>V<sub>3</sub>O<sub>8</sub>, which showed a remarkable specific capacity along with high discharge capacity. In addition to high capacity retention, the monodispersed V<sub>2</sub>O<sub>5</sub> spheres showed a promising discharge capacity. Cu-CTAB-2 displayed excellent discharge capacity and remarkable capacity retention. This material has the highest energy density and a promising cycle life. CuS and Cu<sub>2</sub>MoS<sub>4</sub> nanowires exhibited notable features to be utilized as cathode materials for MIBs. Among Mg<sup>2+</sup>-containing cathode materials, SnO<sub>2</sub>-rGO showed promising characteristics and also paved the way for the development of cathode materials for MIBs. This Review is also supported by the DFT studies of the cathode materials, as first-principles calculations are better alternatives to complex experiments. Among reported cathode materials based on DFT studies, the G-BNyen monolayer has the highest theoretical capacity followed by QHHTP-DPB. However, the long-term stability of the electrode–electrolyte interface is the major problem for the high-voltage electrochemical operation of the electrode materials in MIBs. To make use of such high-voltage cathode materials, it is necessary to find electrolytes or electrolyte additives that are electrochemically stable at high voltage.

Currently, cathode materials for MIBs are a hot topic. Many similar studies are now being conducted; however, describing them would go beyond the scope of this Review. We believe MIBs to be a potential new system for energy storage applications. Particularly, in the case of cathode materials, we hope our Review will encourage researchers to give MIBs their full attention.

## AUTHOR INFORMATION

### Corresponding Authors

**Afzal Shah** – Department of Chemistry, Quaid-I-Azam University, Islamabad 45320, Pakistan; [orcid.org/0000-0002-9465-9185](https://orcid.org/0000-0002-9465-9185); Email: [afzals\\_qau@yahoo.com](mailto:afzals_qau@yahoo.com)

**Iltaf Shah** – Department of Chemistry, College of Science, United Arab Emirates University, Al Ain, Abu Dhabi, United Arab Emirates; Email: [altafshah@uaeu.ac.ae](mailto:altafshah@uaeu.ac.ae)

### Authors

**Mohsin Javed** – Department of Chemistry, Quaid-I-Azam University, Islamabad 45320, Pakistan

**Jan Nisar** – National Centre of Excellence in Physical Chemistry, University of Peshawar, Peshawar 25120, Pakistan; [orcid.org/0000-0001-9291-6064](https://orcid.org/0000-0001-9291-6064)

**Suniya Shahzad** – Department of Chemistry, Quaid-I-Azam University, Islamabad 45320, Pakistan

**Abdul Haleem** – School of Chemistry and Chemical Engineering, Jiangsu University, Zhenjiang, Jiangsu 212013, China; [orcid.org/0000-0003-4034-6498](https://orcid.org/0000-0003-4034-6498)

Complete contact information is available at: <https://pubs.acs.org/10.1021/acsomega.3c06576>

## Notes

The authors declare no competing financial interest.

## ACKNOWLEDGMENTS

We are thankful to Quaid-I-Azam University Islamabad and Higher Education Commission of Pakistan for supporting this work. Authors gratefully acknowledge the support of Research and Sponsored Projects Office, UPAR Grant 12S091, UAE University, UAE.

## REFERENCES

- (1) Ritchie, H. The world population is changing: For the first time there are more people over 64 than children younger than 5. *Age Structure*. Our World in Data, 2023. <https://ourworldindata.org/age-structure>
- (2) Xuan, D.; Jiang, X.; Fang, Y. Can globalization and the green economy hedge natural resources? Functions of population growth and financial development in BRICS countries. *Resour. Policy* 2023, 82, 103414.
- (3) Olabi, A. Renewable energy and energy storage systems. *Energy* 2017, 136, 1–6.
- (4) Khezri, M.; Karimi, M. S.; Mamkhezri, J.; Ghazal, R.; Blank, L. Assessing the impact of selected determinants on renewable energy sources in the electricity mix: The case of ASEAN countries. *Energies* 2022, 15, 4604.
- (5) Asif, M.; Salman, M. U.; Anwar, S.; Gul, M.; Aslam, R. Renewable and non-renewable energy resources of Pakistan and their applicability under the current scenario in Pakistan. *OPEC Energy Rev.* 2022, 46, 310–339.
- (6) Ang, T.-Z.; Salem, M.; Kamarol, M.; Das, H. S.; Nazari, M. A.; Prabakaran, N. A comprehensive study of renewable energy sources: Classifications, challenges and suggestions. *Energy Strategy Rev.* 2022, 43, 100939.
- (7) Qazi, A.; Hussain, F.; Rahim, N. A.; Hardaker, G.; Alghazzawi, D.; Shaban, K.; Haruna, K. Towards sustainable energy: a systematic review of renewable energy sources, technologies, and public opinions. *IEEE access* 2019, 7, 63837–63851.
- (8) Mitali, J.; Dhinakaran, S.; Mohamad, A. Energy storage systems: A review. *Energy Storage Sav.* 2022, 1, 166.
- (9) Hossain, E.; Faruque, H. M. R.; Sunny, M. S. H.; Mohammad, N.; Nawar, N. A comprehensive review on energy storage systems: Types, comparison, current scenario, applications, barriers, and potential solutions, policies, and future prospects. *Energies* 2020, 13, 3651.
- (10) Yang, Y.; Bremner, S.; Menictas, C.; Kay, M. Battery energy storage system size determination in renewable energy systems: A review. *Renewable Sustainable Energy Rev.* 2018, 91, 109–125.
- (11) Winter, M.; Brodd, R. J. What are batteries, fuel cells, and supercapacitors? *Chem. Rev.* 2004, 104, 4245–4270.
- (12) Ometov, A.; Shubina, V.; Klus, L.; Skibińska, J.; Saafi, S.; Pascacio, P.; Flueratoru, L.; Gaibor, D. Q.; Chukhno, N.; Chukhno, O.; et al. A survey on wearable technology: History, state-of-the-art and current challenges. *Comput. Networks* 2021, 193, 108074.
- (13) Kalair, A.; Abas, N.; Saleem, M. S.; Kalair, A. R.; Khan, N. Role of energy storage systems in energy transition from fossil fuels to renewables. *Energy Storage* 2021, 3, No. e135.
- (14) Lund, P. D.; Lindgren, J.; Mikkola, J.; Salpakari, J. Review of energy system flexibility measures to enable high levels of variable renewable electricity. *Renewable Sustainable Energy Rev.* 2015, 45, 785–807.
- (15) Zheng, Y.; He, X.; Wang, H.; Wang, M.; Zhang, S.; Ma, D.; Wang, B.; Wu, Y. Well-to-wheels greenhouse gas and air pollutant emissions from battery electric vehicles in China. *Mitigation Adapt. Strategies Global Change* 2020, 25, 355–370.
- (16) Wells, C.; Minunno, R.; Chong, H.-Y.; Morrison, G. M. Strategies for the adoption of hydrogen-based energy storage systems: an exploratory study in Australia. *Energies* 2022, 15, 6015.

- (17) Tie, S. F.; Tan, C. W. A review of energy sources and energy management system in electric vehicles. *Renewable Sustainable Energy Rev.* **2013**, *20*, 82–102.
- (18) Olabi, A.; Abdelkareem, M. A.; Wilberforce, T.; Alkhalidi, A.; Salameh, T.; Abo-Khalil, A. G.; Hassan, M. M.; Sayed, E. T. Battery electric vehicles: Progress, power electronic converters, strength (S), weakness (W), opportunity (O), and threats (T). *Int. J. Thermofluids* **2022**, *16*, 100212.
- (19) Liu, Z.; Song, J.; Kubal, J.; Susarla, N.; Knehr, K. W.; Islam, E.; Nelson, P.; Ahmed, S. Comparing total cost of ownership of battery electric vehicles and internal combustion engine vehicles. *Energy Policy* **2021**, *158*, 112564.
- (20) Zhao, Y.; Pohl, O.; Bhatt, A. I.; Collis, G. E.; Mahon, P. J.; R  ther, T.; Hollenkamp, A. F. A review on battery market trends, second-life reuse, and recycling. *Sustain. Chem.* **2021**, *2*, 167–205.
- (21) Xu, J.; Thomas, H. R.; Francis, R. W.; Lum, K. R.; Wang, J.; Liang, B. A review of processes and technologies for the recycling of lithium-ion secondary batteries. *J. Power Sources* **2008**, *177*, 512–527.
- (22) Zeng, X.; Li, M.; Abd El-Hady, D.; Alshitari, W.; Al-Bogami, A. S.; Lu, J.; Amine, K. Commercialization of lithium battery technologies for electric vehicles. *Adv. Energy Mater.* **2019**, *9*, 1900161.
- (23) Diouf, B.; Pode, R. Potential of lithium-ion batteries in renewable energy. *Renewable Energy* **2015**, *76*, 375–380.
- (24) Shahjalal, M.; Shams, T.; Islam, M. E.; Alam, W.; Modak, M.; Hossain, S. B.; Ramadesigan, V.; Ahmed, M. R.; Ahmed, H.; Iqbal, A. A review of thermal management for Li-ion batteries: Prospects, challenges, and issues. *J. Energy Storage* **2021**, *39*, 102518.
- (25) Kong, L.; Li, C.; Jiang, J.; Pecht, M. G. Li-ion battery fire hazards and safety strategies. *Energies* **2018**, *11*, 2191.
- (26) Chombo, P. V.; Laoonual, Y. A review of safety strategies of a Li-ion battery. *J. Power Sources* **2020**, *478*, 228649.
- (27) Mallick, S.; Gayen, D. Thermal behaviour and thermal runaway propagation in lithium-ion battery systems-A critical review. *J. Energy Storage* **2023**, *62*, 106894.
- (28) Deng, D. Li-ion batteries: basics, progress, and challenges. *Energy Sci. Eng.* **2015**, *3*, 385–418.
- (29) Ponnada, S.; Kiai, M. S.; Krishnapriya, R.; Singhal, R.; Sharma, R. K. Lithium-free batteries: needs and challenges. *Energy Fuels* **2022**, *36*, 6013–6026.
- (30) Zhang, Z.; Dong, S.; Cui, Z.; Du, A.; Li, G.; Cui, G. Rechargeable magnesium batteries using conversion-type cathodes: A perspective and minireview. *Small Methods* **2018**, *2*, 1800020.
- (31) Fan, E.; Li, L.; Wang, Z.; Lin, J.; Huang, Y.; Yao, Y.; Chen, R.; Wu, F. Sustainable recycling technology for Li-ion batteries and beyond: challenges and future prospects. *Chem. Rev.* **2020**, *120*, 7020–7063.
- (32) Mondal, A.; Das, H. T., Energy storage batteries: basic feature and applications. In *Ceramic Science and Engineering*; Elsevier Series on Advanced Ceramic Materials; Elsevier, 2022; pp 323–351.
- (33) DuChanois, R. M.; Cooper, N. J.; Lee, B.; Patel, S. K.; Mazurowski, L.; Graedel, T. E.; Elimelech, M. Prospects of metal recovery from wastewater and brine. *Nat. Water* **2023**, *1*, 37–46.
- (34) Lukatskaya, M. R.; Dunn, B.; Gogotsi, Y. Multidimensional materials and device architectures for future hybrid energy storage. *Nat. Commun.* **2016**, *7*, 12647.
- (35) Liang, Y.; Dong, H.; Aurbach, D.; Yao, Y. Current status and future directions of multivalent metal-ion batteries. *Nat. Energy* **2020**, *5*, 646–656.
- (36) Bimenyimana, E. The role of renewable energy and battery technology for sustainable electric mobility. Master's Dissertation, University of Rwanda, Kigali, Rwanda, 2020.
- (37) Chen, L.; Bao, J.; Dong, X.; Truhlar, D.; Wang, Y.; Wang, C.; Xia, Y. Aqueous Mg-ion battery based on polyimide anode and prussian blue cathode. *ACS Energy Lett.* **2017**, *2*, 1115–1121.
- (38) Sun, X.; Duffort, V.; Mehdi, B. L.; Browning, N. D.; Nazar, L. F. Investigation of the mechanism of Mg insertion in birnessite in nonaqueous and aqueous rechargeable Mg-ion batteries. *Chem. Mater.* **2016**, *28*, 534–542.
- (39) Shao, Y.; Gu, M.; Li, X.; Nie, Z.; Zuo, P.; Li, G.; Liu, T.; Xiao, J.; Cheng, Y.; Wang, C.; et al. Highly reversible Mg insertion in nanostructured Bi for Mg ion batteries. *Nano Lett.* **2014**, *14*, 255–260.
- (40) Huie, M. M.; Bock, D. C.; Takeuchi, E. S.; Marschilok, A. C.; Takeuchi, K. J. Cathode materials for magnesium and magnesium-ion based batteries. *Coord. Chem. Rev.* **2015**, *287*, 15–27.
- (41) Li, C.; Lin, L.; Wu, W.; Sun, X. A High Potential Polyanion Cathode Material for Rechargeable Mg-Ion Batteries. *Small Methods* **2022**, *6*, 2200363.
- (42) Xu, Y.; Deng, X.; Li, Q.; Zhang, G.; Xiong, F.; Tan, S.; Wei, Q.; Lu, J.; Li, J.; An, Q.; et al. Vanadium oxide pillared by interlayer Mg<sup>2+</sup> ions and water as ultralong-life cathodes for magnesium-ion batteries. *Chem* **2019**, *5*, 1194–1209.
- (43) Ma, Z.; MacFarlane, D. R.; Kar, M. Mg cathode materials and electrolytes for rechargeable Mg batteries: a review. *Batteries Supercaps* **2019**, *2*, 115–127.
- (44) Levi, E.; Gofer, Y.; Aurbach, D. On the way to rechargeable Mg batteries: the challenge of new cathode materials. *Chem. Mater.* **2010**, *22*, 860–868.
- (45) Pryke, J. J.; Kennard, R. M.; Cussen, S. A. Cathodes for Mg batteries: A condensed review. *Energy Rep.* **2022**, *8*, 83–88.
- (46) Aurbach, D.; Lu, Z.; Schechter, A.; Gofer, Y.; Gizbar, H.; Turgeman, R.; Cohen, Y.; Moshkovich, M.; Levi, E. Prototype systems for rechargeable magnesium batteries. *Nature* **2000**, *407* (6805), 724–727.
- (47) Zhao-Karger, Z.; Fichtner, M. Beyond intercalation chemistry for rechargeable Mg batteries: a short review and perspective. *Front. Chem.* **2019**, *6*, 656.
- (48) Wrogegmann, J. M.; Rodr  guez-P  rez, I. A.; Winter, M.; Placke, T. Contribution of nano-design approaches to future electrochemical energy storage systems. *Front. Nanosci.* **2021**, *19*, 273–325.
- (49) Wang, Z.; Jiang, H.; Zhang, Y.; An, Y.; Wei, C.; Tan, L.; Xiong, S.; Qian, Y.; Feng, J. Application of 2D MXene in Organic Electrode Materials for Rechargeable Batteries: Recent Progress and Perspectives. *Adv. Funct. Mater.* **2023**, *33*, 2210184.
- (50) Yan, C.; Xu, R.; Xiao, Y.; Ding, J. F.; Xu, L.; Li, B. Q.; Huang, J. Q. Toward critical electrode/electrolyte interfaces in rechargeable batteries. *Adv. Funct. Mater.* **2020**, *30*, 1909887.
- (51) Al-Samet, M. A.; Burgaz, E. Improving the lithium-ion diffusion and electrical conductivity of LiFePO<sub>4</sub> cathode material by doping magnesium and multi-walled carbon nanotubes. *J. Alloys Compd.* **2023**, *947*, 169680.
- (52) Islam, M. S.; Mubarak, M.; Lee, H.-J. Hybrid Nanostructured Materials as Electrodes in Energy Storage Devices. *Inorganics* **2023**, *11*, 183.
- (53) Boz, B.; Dev, T.; Salvadori, A.; Schaefer, J. L. Electrolyte and electrode designs for enhanced ion transport properties to enable high performance lithium batteries. *J. Electrochem. Soc.* **2021**, *168*, 090501.
- (54) Cheong, J. Y.; Cho, S. H.; Lee, J.; Jung, J. W.; Kim, C.; Kim, I. D. Multifunctional 1D nanostructures toward future batteries: A comprehensive review. *Adv. Funct. Mater.* **2022**, *32*, 2208374.
- (55) Baig, N.; Kammakam, I.; Falath, W. Nanomaterials: A review of synthesis methods, properties, recent progress, and challenges. *Mater. Adv.* **2021**, *2*, 1821–1871.
- (56) Yu, L.; Zhou, X.; Lu, L.; Wu, X.; Wang, F. Recent Developments of Nanomaterials and Nanostructures for High-Rate Lithium Ion Batteries. *ChemSusChem* **2020**, *13*, 5361–5407.
- (57) Liu, W.; Placke, T.; Chau, K. Overview of batteries and battery management for electric vehicles. *Energy Rep.* **2022**, *8*, 4058–4084.
- (58) Duehnen, S.; Betz, J.; Kolek, M.; Schmuck, R.; Winter, M.; Placke, T. Toward green battery cells: Perspective on materials and technologies. *Small Methods* **2020**, *4* (7), 2000039.
- (59) Zhang, R.; Yu, X.; Nam, K.-W.; Ling, C.; Arthur, T. S.; Song, W.; Knapp, A. M.; Ehrlich, S. N.; Yang, X.-Q.; Matsui, M.  $\alpha$ -MnO<sub>2</sub> as a cathode material for rechargeable Mg batteries. *Electrochem. Commun.* **2012**, *23*, 110–113.
- (60) Rasul, S.; Suzuki, S.; Yamaguchi, S.; Miyayama, M. Synthesis and electrochemical behavior of hollandite MnO<sub>2</sub>/acetylene black

composite cathode for secondary Mg-ion batteries. *Solid State Ionics* **2012**, *225*, 542–546.

(61) Wang, L.; Asheim, K.; Vullum, P. E.; Svensson, A. M.; Vullum-Bruer, F. Sponge-like porous manganese (II, III) oxide as a highly efficient cathode material for rechargeable magnesium ion batteries. *Chem. Mater.* **2016**, *28*, 6459–6470.

(62) Van Vy, U.; Que, L. X. Study on fabrication of MnO<sub>2</sub>/CNTs composite by electrolysis in neutral solution and its applicability as cathode materials in Mg-ion batteries. *Vietnam J. Chem.* **2021**, *59*, 494–499.

(63) Nam, K. W.; Kim, S.; Lee, S.; Salama, M.; Shterenberg, I.; Gofer, Y.; Kim, J.-S.; Yang, E.; Park, C. S.; Kim, J.-S.; et al. The high performance of crystal water containing manganese birnessite cathodes for magnesium batteries. *Nano Lett.* **2015**, *15*, 4071–4079.

(64) Liu, B.; Luo, T.; Mu, G.; Wang, X.; Chen, D.; Shen, G. Rechargeable Mg-ion batteries based on WSe<sub>2</sub> nanowire cathodes. *ACS Nano* **2013**, *7*, 8051–8058.

(65) Wei, L.; Lian, R.; Zhao, Y.; Meng, Y.; He, L.; Yu, Y.; Chen, G.; Wei, Y. Experimental investigation and first-principles calculations of a Ni<sub>3</sub>Se<sub>4</sub> cathode material for Mg-ion batteries. *ACS Appl. Mater. Interfaces* **2020**, *12*, 9316–9321.

(66) Xu, J.; Wei, Z.; Zhang, S.; Wang, X.; Wang, Y.; He, M.; Huang, K. Hierarchical WSe<sub>2</sub> nanoflower as a cathode material for rechargeable Mg-ion batteries. *J. Colloid Interface Sci.* **2021**, *588*, 378–383.

(67) Gao, Y.-p.; Zhai, Z.; Dong, Y.; Pang, Y.; Chen, J.; Li, G. 1 T-VSe<sub>2</sub> Nanoparticles cooperated with reduced graphene oxide as a superior cathode material for rechargeable Mg-ion batteries. *Appl. Surf. Sci.* **2022**, *592*, 153141.

(68) Shen, Y.; Wang, Y.; Miao, Y.; Li, Q.; Zhao, X.; Shen, X. Anion-Incorporated Mg-Ion Solvation Modulation Enables Fast Magnesium Storage Kinetics of Conversion-Type Cathode Materials. *Adv. Mater.* **2023**, *35*, 2208289.

(69) Tashiro, Y.; Taniguchi, K.; Miyasaka, H. Copper selenide as a new cathode material based on displacement reaction for rechargeable magnesium batteries. *Electrochim. Acta* **2016**, *210*, 655–661.

(70) Kim, R.-H.; Kim, J.-S.; Kim, H.-J.; Chang, W.-S.; Han, D.-W.; Lee, S.-S.; Doo, S.-G. Highly reduced VO<sub>x</sub> nanotube cathode materials with ultra-high capacity for magnesium ion batteries. *J. Mater. Chem. A* **2014**, *2*, 20636–20641.

(71) Tepavcevic, S.; Liu, Y.; Zhou, D.; Lai, B.; Maser, J.; Zuo, X.; Chan, H.; Král, P.; Johnson, C. S.; Stamenkovic, V.; et al. Nanostructured layered cathode for rechargeable Mg-ion batteries. *ACS Nano* **2015**, *9*, 8194–8205.

(72) Sheha, E.; Makled, M.; Nouman, W. M.; Bassyouni, A.; Yaghamour, S.; Abo-Elhassan, S. Vanadium Oxide/graphene nanoplatelet as a cathode material for Mg-ion battery. *Graphene* **2016**, *05*, 178.

(73) Fu, Q.; Sarapulova, A.; Trouillet, V.; Zhu, L.; Fauth, F.; Mangold, S.; Welter, E.; Indris, S.; Knapp, M.; Dsoke, S.; et al. In operando synchrotron diffraction and in operando X-ray absorption spectroscopy investigations of orthorhombic V<sub>2</sub>O<sub>5</sub> nanowires as cathode materials for Mg-ion batteries. *J. Am. Chem. Soc.* **2019**, *141*, 2305–2315.

(74) Mukherjee, A.; Taragin, S.; Aviv, H.; Perelshtein, I.; Noked, M. Rationally designed vanadium pentoxide as high capacity insertion material for Mg-ion. *Adv. Funct. Mater.* **2020**, *30*, 2003518.

(75) Fu, Q.; Wu, X.; Luo, X.; Indris, S.; Sarapulova, A.; Bauer, M.; Wang, Z.; Knapp, M.; Ehrenberg, H.; Wei, Y.; et al. High-Voltage Aqueous Mg-Ion Batteries Enabled by Solvation Structure Reorganization. *Adv. Funct. Mater.* **2022**, *32*, 2110674.

(76) Rastgoo-Deylami, M.; Chae, M. S.; Hong, S.-T. H<sub>2</sub>V<sub>3</sub>O<sub>8</sub> as a high energy cathode material for nonaqueous magnesium-ion batteries. *Chem. Mater.* **2018**, *30*, 7464–7472.

(77) Ji, X.; Chen, J.; Wang, F.; Sun, W.; Ruan, Y.; Miao, L.; Jiang, J.; Wang, C. Water-activated VOPO<sub>4</sub> for magnesium ion batteries. *Nano Lett.* **2018**, *18*, 6441–6448.

(78) Esparcia Jr, E. A.; Chae, M. S.; Ocon, J. D.; Hong, S.-T. Ammonium vanadium bronze (NH<sub>4</sub>V<sub>4</sub>O<sub>10</sub>) as a high-capacity

cathode material for nonaqueous magnesium-ion batteries. *Chem. Mater.* **2018**, *30*, 3690–3696.

(79) Zuo, C.; Tang, W.; Lan, B.; Xiong, F.; Tang, H.; Dong, S.; Zhang, W.; Tang, C.; Li, J.; Ruan, Y.; et al. Unexpected discovery of magnesium-vanadium spinel oxide containing extractable Mg<sup>2+</sup> as a high-capacity cathode material for magnesium ion batteries. *Chem. Eng. J.* **2021**, *405*, 127005.

(80) Ma, X.-F.; Li, H.-Y.; Gao, D.; Ren, W.; Diao, J.; Xie, B.; Huang, G.; Wang, J.; Pan, F. Mg<sub>3</sub>V<sub>2</sub>O<sub>8</sub>: A Promising Cathode Material for Aqueous Mg-ion Battery. In *Magnesium Technology 2023*; Springer, 2023; pp 219–224.

(81) Ma, X. F.; Li, H. Y.; Zhu, X.; Ren, W.; Zhang, X.; Diao, J.; Xie, B.; Huang, G.; Wang, J.; Pan, F. Switchable and Strain-Releasable Mg-Ion Diffusion Nanohighway Enables High-Capacity and Long-Life Pyrovanadate Cathode. *Small* **2022**, *18*, 2202250.

(82) Inamoto, M.; Kurihara, H.; Yajima, T. Vanadium pentoxide-based composite synthesized using microwave water plasma for cathode material in rechargeable magnesium batteries. *Materials* **2013**, *6*, 4514–4522.

(83) Canepa, P.; Sai Gautam, G.; Hannah, D. C.; Malik, R.; Liu, M.; Gallagher, K. G.; Persson, K. A.; Ceder, G. Odyssey of multivalent cathode materials: open questions and future challenges. *Chem. Rev.* **2017**, *117*, 4287–4341.

(84) Kravchyk, K. V.; Widmer, R.; Erni, R.; Dubey, R. J.-C.; Krumeich, F.; Kovalenko, M. V.; Bodnarchuk, M. I. Copper sulfide nanoparticles as high-performance cathode materials for Mg-ion batteries. *Sci. Rep.* **2019**, *9*, 7988.

(85) Le, L. T.; Truong, D. Q.; Ung, T. T.; Nguyen, L. H.; Vu, L. D.; Tran, P. D. Cu<sub>2</sub>MoS<sub>4</sub> Nanotubes as a Cathode Material for Rechargeable Magnesium-ion Battery. *ChemistrySelect* **2020**, *5*, 280–283.

(86) Shen, Y.; Wang, Y.; Miao, Y.; Yang, M.; Zhao, X.; Shen, X. High-energy interlayer-expanded copper sulfide cathode material in non-corrosive electrolyte for rechargeable magnesium batteries. *Adv. Mater.* **2020**, *32*, 1905524.

(87) Chen, D.; Tao, D.; Ren, X.; Wen, F.; Li, T.; Chen, Z.; Cao, Y.; Xu, F. A Molybdenum Polysulfide In-Situ Generated from Ammonium Tetrathiomolybdate for High-Capacity and High-Power Rechargeable Magnesium Battery Cathodes. *ACS Nano* **2022**, *16*, 20510–20520.

(88) Liang, Y.; Feng, R.; Yang, S.; Ma, H.; Liang, J.; Chen, J. Rechargeable Mg batteries with graphene-like MoS<sub>2</sub> cathode and ultrasmall Mg nanoparticle anode. *Adv. Mater.* **2011**, *23*, 640–643.

(89) Truong, Q. D.; Devaraju, M. K.; Honma, I. Nanocrystalline MgMnSiO<sub>4</sub> and MgCoSiO<sub>4</sub> particles for rechargeable Mg-ion batteries. *J. Power Sources* **2017**, *361*, 195–202.

(90) Heath, J.; Chen, H.; Islam, M. S. MgFeSiO<sub>4</sub> as a potential cathode material for magnesium batteries: ion diffusion rates and voltage trends. *J. Mater. Chem. A* **2017**, *5*, 13161–13167.

(91) Mao, M.; Gao, T.; Hou, S.; Wang, C. A critical review of cathodes for rechargeable Mg batteries. *Chem. Soc. Rev.* **2018**, *47*, 8804–8841.

(92) Truong, Q. D.; Kempaiah Devaraju, M.; Tran, P. D.; Gambe, Y.; Nayuki, K.; Sasaki, Y.; Honma, I. Unravelling the surface structure of MgMn<sub>2</sub>O<sub>4</sub> cathode materials for rechargeable magnesium-ion battery. *Chem. Mater.* **2017**, *29*, 6245–6251.

(93) Kobayashi, H.; Yamaguchi, K.; Honma, I. Rapid room-temperature synthesis of ultrasmall cubic Mg-Mn spinel cathode materials for rechargeable Mg-ion batteries. *RSC Adv.* **2019**, *9*, 36434–36439.

(94) Kwon, B. J.; Yin, L.; Park, H.; Parajuli, P.; Kumar, K.; Kim, S.; Yang, M.; Murphy, M.; Zapol, P.; Liao, C.; et al. High voltage Mg-ion battery cathode via a solid solution Cr-Mn spinel oxide. *Chem. Mater.* **2020**, *32*, 6577–6587.

(95) Zhang, Y.; Liu, G.; Zhang, C.; Chi, Q.; Zhang, T.; Feng, Y.; Zhu, K.; Zhang, Y.; Chen, Q.; Cao, D. Low-cost MgFe<sub>x</sub>Mn<sub>2-x</sub>O<sub>4</sub> cathode materials for high-performance aqueous rechargeable magnesium-ion batteries. *Chem. Eng. J.* **2020**, *392*, 123652.



- (96) Yokozaki, R.; Kobayashi, H.; Honma, I. Reductive solvothermal synthesis of  $\text{MgMn}_2\text{O}_4$  spinel nanoparticles for Mg-ion battery cathodes. *Ceram. Int.* **2021**, *47*, 10236–10241.
- (97) Asif, M.; Rashad, M.; Shah, J. H.; Zaidi, S. D. A. Surface modification of tin oxide through reduced graphene oxide as a highly efficient cathode material for magnesium-ion batteries. *J. Colloid Interface Sci.* **2020**, *561*, 818–828.
- (98) Javadian, S.; Ghavam, S. J.; Dalir, N.; Gharibi, H. Template-based design hollow spheres spinel and reduce graphene oxide composite as a super stable cathode for aqueous Mg-ion battery. *Mater. Chem. Phys.* **2022**, *284*, 126050.
- (99) Hatakeyama, T.; Li, H.; Okamoto, N. L.; Shimokawa, K.; Kawaguchi, T.; Tanimura, H.; Imashuku, S.; Fichtner, M.; Ichitsubo, T. Accelerated kinetics revealing metastable pathways of magnesia-ion-induced transformations in  $\text{MnO}_2$  polymorphs. *Chem. Mater.* **2021**, *33* (17), 6983–6996.
- (100) Okamoto, S.; Ichitsubo, T.; Kawaguchi, T.; Kumagai, Y.; Oba, F.; Yagi, S.; Shimokawa, K.; Goto, N.; Doi, T.; Matsubara, E. Intercalation and Push-Out Process with Spinel-to-Rocksalt Transition on Mg Insertion into Spinel Oxides in Magnesium Batteries. *Adv. Sci.* **2015**, *2* (8), 1500072.
- (101) Jain, A.; Shin, Y.; Persson, K. A. Computational predictions of energy materials using density functional theory. *Nat. Rev. Mater.* **2016**, *1*, 15004.
- (102) Bryenton, K. R.; Adeleke, A. A.; Dale, S. G.; Johnson, E. R. Delocalization error: The greatest outstanding challenge in density-functional theory. *Wiley Interdiscip. Rev.: Comput. Mol. Sci.* **2023**, *13*, No. e1631.
- (103) Tian, C.; Li, T.; Bustillos, J.; Bhattacharya, S.; Turnham, T.; Yeo, J.; Moridi, A. Data-Driven Approaches Toward Smarter Additive Manufacturing. *Adv. Intell. Syst.* **2021**, *3*, 2100014.
- (104) Lunghi, A.; Sanvito, S. Computational design of magnetic molecules and their environment using quantum chemistry, machine learning and multiscale simulations. *Nat. Rev. Chem.* **2022**, *6*, 761–781.
- (105) Yang, J.; Wang, J.; Dong, X.; Zhu, L.; Hou, D.; Zeng, W.; Wang, J. The potential application of  $\text{VS}_2$  as an electrode material for Mg ion battery: A DFT study. *Appl. Surf. Sci.* **2021**, *544*, 148775.
- (106) He, Q.; Yu, B.; Li, Z.; Zhao, Y. Density functional theory for battery materials. *Energy Environ. Mater.* **2019**, *2*, 264–279.
- (107) Juran, T. R.; Young, J.; Smeu, M. Density functional theory modeling of  $\text{MnO}_2$  polymorphs as cathodes for multivalent ion batteries. *J. Phys. Chem. C* **2018**, *122*, 8788–8795.
- (108) Bursch, M.; Mewes, J. M.; Hansen, A.; Grimme, S. Best-Practice DFT Protocols for Basic Molecular Computational Chemistry. *Angew. Chem. Int. Ed.* **2022**, *61*, No. e202205735.
- (109) Chen, B. W.; Xu, L.; Mavrikakis, M. Computational methods in heterogeneous catalysis. *Chem. Rev.* **2021**, *121*, 1007–1048.
- (110) Pavošević, F.; Culpitt, T.; Hammes-Schiffer, S. Multi-component quantum chemistry: Integrating electronic and nuclear quantum effects via the nuclear-electronic orbital method. *Chem. Rev.* **2020**, *120* (9), 4222–4253.
- (111) Al-Mahayni, H.; Wang, X.; Harvey, J. P.; Patience, G. S.; Seifitokaldani, A. Experimental methods in chemical engineering: Density functional theory. *Can. J. Chem. Eng.* **2021**, *99* (9), 1885–1911.
- (112) Yeo, P. S. E.; Ng, M.-F. First-principles study of molybdenum chalcogenide halide nanowires for Mg-ion battery cathode application. *Chem. Mater.* **2015**, *27*, 5878–5885.
- (113) Shan, P.; Gu, Y.; Yang, L.; Liu, T.; Zheng, J.; Pan, F. Olivine  $\text{FePO}_4$  cathode material for rechargeable Mg-ion batteries. *Inorg. Chem.* **2017**, *56*, 13411–13416.
- (114) Shasha, H.; Yatom, N.; Prill, M.; Zaffran, J.; Biswas, S.; Aurbach, D.; Toroker, M. C.; Ein-Eli, Y. Unveiling ionic diffusion in  $\text{MgNiMnO}_4$  cathode material for Mg-ion batteries via combined computational and experimental studies. *J. Solid State Electrochem.* **2019**, *23*, 3209–3216.
- (115) Kulik, H. J. Treating electron over-delocalization with the DFT+U method. *J. Chem. Phys.* **2015**, *142*, 240901.
- (116) Ahn, E. G.; Yang, J.-H.; Lee, J.-H.  $\text{Mg}_3\text{Si}_3(\text{MoO}_6)_2$  as a High-Performance Cathode Active Material for Magnesium-Ion Batteries. *ACS Appl. Mater. Interfaces* **2021**, *13*, 47749–47755.
- (117) Khan, A. A.; Muhammad, I.; Ahmad, R.; Ahmad, I.; Ullah, N. First principle study of benzoquinone based microporous conjugated polymers as cathode materials for high-performance magnesium ion batteries. *Comput. Mater. Sci.* **2022**, *214*, 111757.
- (118) Yang, J.; Wang, J.; Wang, X.; Dong, X.; Zhu, L.; Zeng, W.; Wang, J.; Pan, F. First-principles prediction of layered  $\text{MoO}_2$  and  $\text{MoOSe}$  as promising cathode materials for magnesium ion batteries. *Nanotechnology* **2021**, *32*, 495405.
- (119) Sivaraman, R.; Patra, I.; Opulencia, M. J. C.; Sagban, R.; Sharma, H.; Jalil, A. T.; Ebadi, A. G. Evaluating the potential of graphene-like boron nitride as a promising cathode for Mg-ion batteries. *J. Electroanal. Chem.* **2022**, *917*, 116413.
- (120) Khan, A. A.; Muhammad, I.; Ahmad, R.; Ahmad, I.; Ullah, N. Quinone functionalized highly porous polymer as cathode material for Mg ion batteries: A DFT study. *J. Power Sources* **2023**, *580*, 233358.